Energy Conversion and Management 291 (2023) 117168

Contents lists available at ScienceDirect

Energy Conversion and Management

journal homepage: www.elsevier.com/locate/enconman

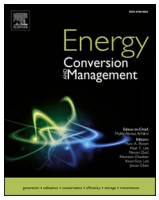

A comprehensive multi-node multi-vector multi-sector modelling framework to investigate integrated energy systems and assess decarbonisation needs

Paolo Colbertaldo *, Federico Parolin, Stefano Campanari

Group of Energy Conversion Systems (GECOS), Department of Energy, Politecnico di Milano – Via Lambruschini 4A, 20156 Milan, Italy

ARTICLE INFO

Keywords:
Energy system modelling
Multi-vector
Net-zero CO_2 emissions
OMNI-ES
Sector coupling

ABSTRACT

The pathway towards decarbonised energy systems involves massive changes in adopted energy vectors, installed technologies, networks roles, and interaction capabilities. To investigate the combination of these effects, this work presents the OMNI-ES modelling framework (Optimisation Model for Network-Integrated Energy Systems), which offers a comprehensive approach to analyse multi-node, multi-vector, multi-sector energy systems. It adopts a detailed temporal and spatial resolution and implements multiple conversion options between energy vectors (electricity, hydrogen, natural gas, biomethane, biofuels, e-fuels, …). The formulation solves the energy vector balances at each time step, taking into account sources, sinks, conversion processes, and storage systems. CO_2 flows are also tracked, allowing the introduction of CO_2 emission constraints that account for all contributions (fossil and biogenic, direct and indirect) and mitigation measures (capture, re-use, sequestration). In the article, OMNI-ES is applied to investigate an Italian scenario for 2050, adopting a regional (NUTS-2) resolution. The model output yields the cost-optimal energy system configuration that is capable to support the demand with net-zero CO_2 emissions. Results show that the need for CO_2 balance closure calls in several technologies, including massive renewable power generation (up to 20 times today's capacities), storage systems (batteries, hydrogen, pumped hydro), biogenic sources (residual biomass and biomethane), and CO_2 capture (both on fossil and biogenic sources). Networks emerge as critical elements, as the need to transport energy vectors saturates the expected capacities of grid infrastructures, especially in the case of hydrogen.

1. Introduction

The achievement of a carbon–neutral society represents an unprecedented challenge in human history, dictating a paradigm-shifting transformation of the energy systems that underpin all economic activities. The magnitude of such an endeavour is impelling governments to take urgent actions, as over a hundred countries worldwide have pledged to reach net-zero CO_2 emissions by mid-century, covering more than 80% of global emissions [1]. Despite the growing political consensus, only few pledges are supported by detailed strategies, and policy-making bodies generally lack a holistic approach to decarbonisation [2].

The pathway to net-zero CO_2 emissions requires coordinated efforts in all the energy-consuming sectors, with a strong integration of processes and energy vectors. To replace fossil fuels, renewable energy sources (RES) are expected to experience a massive deployment, making the power generation sector a decarbonisation forerunner. According to prevailing scenarios, renewable-based power generation will pave the way for a widespread electrification across all demand sectors, which has the twofold advantage of cutting emissions and improving energy efficiency [3]. The development of energy storage systems is crucial to enable RES penetration, given that the most abundant sources, solar and wind, are intrinsically intermittent and non-dispatchable. Among the possible solutions, battery energy storage systems (BESS) appear crucial to manage high overgeneration peaks, while Power-to-Hydrogen (P2H) is emerging as a key technology to perform seasonal storage, by converting surplus electricity into chemical energy. Different pathways can be envisaged for the produced hydrogen, as it can be reconverted into electricity (Power-to-Power, P2P), used in pure form, or converted into liquid fuels (Power-to-Liquid, P2L), enabling the decarbonisation of processes and activities for which direct electrification is impractical [4].

The decarbonisation of all demand sectors can be achieved only

* Corresponding author.
E-mail address: paolo.colbertaldo@polimi.it (P. Colbertaldo).

https://doi.org/10.1016/j.enconman.2023.117168

Available online 14 June 2023

Nomenclature

Acronyms and abbreviations

BESS	Battery energy storage systems
BEV	Battery electric vehicle
BTX	Benzene, toluene, and xylenes
CAPEX	Capital expenditure
CCGT	Combined-cycle gas turbine
CCS	Carbon capture and storage
COP	Coefficient of performance
CRF	Capital recovery factor
DAC	Direct air capture
DRI	Direct reduction of iron ore
EAF	Electric arc furnace
EE	Electric energy
ESM	Energy system model
FC	Fuel cell
FCEV	Fuel cell electric vehicle
GDP	Gross domestic product
GT	Gas turbine
HDD	Heating degree days
HP	Heat pump
HVC	High value chemicals
ICEV	Internal combustion engine vehicle
LF	Liquid fuels
LH_2	Liquid hydrogen
LHV	Lower heating value
LNG	Liquefied natural gas
LP	Linear programming
LPG	Liquefied petroleum gas
LTS	Long-term strategy
MGA	Modelling to generate alternatives
NECP	National Energy and Climate Plan
NG	Natural gas
O&M	Operation and maintenance
OCGT	Open-cycle gas turbine
OMNI-ES	Optimisation Model for Network-Integrated Energy Systems
OPEX	Operational expenditure
P2H	Power-to-Hydrogen
P2L	Power-to-Liquid
P2P	Power-to-Power
PHS	Pumped hydro storage
PV	Photovoltaic
RES	Renewable energy sources
SMR	Steam methane reforming
TAC	Total annual cost
TSO	Transmission system operator
WtE	Waste-to-Energy

Subscripts

bes	Battery energy storage systems
BFp	Biofuel production (in: biomass; out: LF)
bms	Biomass
bmt	Biomethane
cgt	Gas turbine combined cycles (in: G; out: EE)
cpt	CO_2 capture (in: EE and CO_2; out: CO_2)
crt	Curtailment
dac	Direct air capture (in: EE and CO_2; out: CO_2)
dem	Final demand
EFp	e-fuel production (in: H_2 and CO_2; out: LF)
elc	Electrolysis (in: EE; out: H_2)
fcs	Fuel cell systems (in: H_2, out: EE)
geo	Geothermal
hyd	Hydroelectric
inj	H_2 injection into gas network (in: H_2; out: G-H_2)
ipt	Input
LB	Lower boundary
NGdom	Domestic NG production
ogt	Gas turbine open cycles (in: G; out: EE)
otp	Output
phs	Pumped hydro storage systems
pvt	Solar photovoltaic
sep	H_2 separation from gas network (in: EE, G-H_2; out: H_2)
smr	Steam methane reforming (in: G-CH_4; out: H_2)
trn	Transport
UB	Upper boundary
wnn	Wind onshore
wno	Wind offshore
wst	Waste
WtE	Waste-to-Energy

Sets

$i \in I$	Generic technology of the energy system
$j \in J$	Generic item of operational expenditures
$k \in K$	End-use sector
$n \in N$	Node of the energy vector networks
$p \in P$	Conversion process
$s_v \in S_v$	Source for energy vector v
$t \in T$	Time step
$v \in V$	Energy vector
$\sigma_v \in \Sigma_v$	Available storage system for energy vector v

Energy vectors

CH_4	Methane
EE	Electric energy
G	Gas (blend CH_4-H_2)
G-CH_4	Methane in gas
G-H_2	Hydrogen in gas
H_2	Hydrogen (pure)
LF	Liquid fuels

Model parameters

$\tilde{C}^{n}_{i,ref}$	Installed capacity of technology i at node n in reference year (MW)
$\tilde{C}^{n}_{i,UB}$	Upper boundary of the installed capacity of technology i at node n (MW)
$\tilde{C}^{n}_{s,UB}$	Upper boundary of the availability of source s at node n (MWh/y)
$\tilde{C}^{n,n'}_{\mathrm{trn},G}$	Transport capacity of the connection between nodes n and n' in the gas network (m^3/h)
$\tilde{c}_{s,v}$	Specific supply cost of source s for the energy vector v (€/MWh)
$\tilde{c}_{\mathrm{trn},v}$	Specific transport cost of energy vector v (€/MWh)
$\tilde{\mathrm{capex}}_i$	Specific CAPEX of technology i (€/MW)
$\tilde{CRF}_i$	Capital recovery factor of technology i (-)
$\tilde{e}_{CO_2,LF}$	CO_2 emission factor of liquid fuels at point of use (t_{CO2}/MWh_{LHV})
$\tilde{e}_{CO_2,NG}$	CO_2 emission factor of natural gas at point of use (t_{CO2}/MWh_{LHV})
$\tilde{e}_{CO_2,wst}$	CO_2 emission factor of waste for incineration at point of use (t_{CO2}/MWh_{LHV})
$\tilde{\mathrm{opex}}_{\%\mathrm{fix},i}$	Specific fixed OPEX of technology i, as percentage of CAPEX (y^{-1})
$\tilde{q}^{n,t}_{\mathrm{dem},k,v}$	Exogenous demand of energy vector v for sector k at node n and time step t

$\tilde{x}_{H_2,max,i}$ Maximum hydrogen fraction allowed in technology i (-)
$\tilde{x}^{n,n'}_{H_2,max,trn}$ Maximum hydrogen fraction allowed in the connection between nodes n and n' in the gas network (-)
$\tilde{\alpha}_{p,v'\rightarrow v}$ Conversion factor of energy vector v' into energy vector v through process p ($MW_v/MW_{v'}$)
$\tilde{\Delta t}$ Time step duration (h)
$\tilde{\varepsilon}_{\sigma,v}$ Self-discharge coefficient of storage technology σ for energy vector v (h^{-1})
$\tilde{\nu}_{CH_4}$ Specific volume on energy basis of methane (m^3/MWh_{LHV})
$\tilde{\eta}_i$ Efficiency of technology i (-)
$\tilde{\nu}_{H_2}$ Specific volume on energy basis of hydrogen (m^3/MWh_{LHV})

Model variables

C^n_i Capacity of technology i at node n (MW)
$CAPEX_i$ Capital expenditure of technology i (€)
FC Total fixed operational costs (€/y)
$OPEX_j$ Generic operational expenditure (€/y)
$OPEX_{var}$ Total variable operational expenditures (€/y)
q_{abs,CO_2} Natural absorption of CO_2 (t_{CO2}/y)
$q^{n,t}_{crt,v}$ Curtailment of energy vector v at node n and time step t (MW)
$q^{n,t}_{dem,G\text{-}CH_4}$ Methane amount in gas end uses at node n and time step t (MW)
$q^{n,t}_{dem,G\text{-}H_2}$ Hydrogen amount in gas end uses at node n and time step t (MW)
q_{ext,CO_2} High-cost balance closure term in the CO_2 emission constraint (t_{CO2}/y)
$q^{n,t}_{i,v}$ Generic flow of energy vector v in technology i at node n and time step t (MW)
$q^{n,t}_{impC,v}$ Import amount of energy vector v with category C at node n and time step t (MW) $v = \{EE, H2, LF\} C = \{BLUE, GREEN, GREY\}$
$q^{n,t}_{impNG,G\text{-}CH_4}$ Natural gas import at node n and time step t (MW_{LHV})
q_{una,CO_2} Unavoidable CO_2 emission (t_{CO2}/y)
$q^{n,t}_{ipt,p,v}$ Input flow of energy vector v in process p at node n and time step t (MW)$p \in P = \{BFp, cpt_i, DAC, EFp, elc, fcs, cgt, ogt, inj, sep, smr\}$
$q^{n,t}_{ipt,\sigma_v,v}$ Input flow of energy vector v in the storage technology σ_v at node n and time step t (MW)
$q^{n,t}_{otp,p,v}$ Output flow of energy vector v from process p at node n and time step t (MW) $p \in P = \{BFp, cpt_i, dac, EFp, elc, fcs, cgt, ogt, inj, sep, smr\}$
$q^{n,t}_{otp,\sigma_v,v}$ Output flow of energy vector v from the storage technology σ at node n and time step t (MW)
$q^{n,t}_{s,v}$ Flow of source s for energy vector v at node n and time step t (MW)
q_{sc,CO_2} Supply chain-related emissions (t_{CO2}/y)
$q^{n,t}_{str,CO_2}$ CO_2 flow to permanent sequestration at node n and time step t (t_{CO2}/h)
$q^{n,n',t}_{trn,v}$ Quantity of energy vector v transported from node n to node n' at time step t (MW)
$Q^{n,t}_{\sigma_v,v}$ Storage content of energy vector v in technology σ_v at node n and time step t (MWh)
TAC Total annual cost
VC Total variable costs

through the synergetic use of different energy vectors and sources, prioritising electrification to benefit from efficiency improvement. The transport sector must undergo a dramatic switch from oil-based fuels to electric drivetrains. In particular, battery electric vehicles (BEVs) are expected to represent the standard for light mobility [3], whereas hydrogen-powered fuel cell electric vehicles (FCEVs) appear preferable for long-haul and heavy-duty transport [4]. Carbon-neutral liquid fuels, hydrogen, and hydrogen derivatives are typically identified as the main decarbonisation options for aviation [5] and navigation [6], since electric propulsion is applicable only for short-haul routes due to battery weight and size. Different roadmaps suggest that energy efficiency improvements and electrification will be the main drivers of the decarbonisation of the residential and services sector, as a massive deployment of heat pumps is expected to replace natural gas (NG)-based heating [3]. Renewable gases, such as hydrogen or biomethane, may represent the alternative to decarbonise buildings in which the installation of heat pumps is not viable [7]. The full electrification of industry might be impractical, since electric technologies for high-grade heat generation are still at low maturity level [8] and various processes require carbon-based feedstocks. The combustion of renewable gases or the implementation of carbon capture and storage (CCS) are viable options to provide decarbonised high-temperature heat [2], while hydrogen and hydrogen-based fuels (e.g., methanol) can be used to replace natural gas and oil-based liquid fuel feedstocks in the chemical industry [9].

1.1. Review of energy system models

To assist policy makers and outline possible pathways, the topic of decarbonisation is typically addressed by developing energy system models (ESMs). The existing literature features numerous examples, and such tools are in continuous development in response to the increasing ambition of climate targets. Various efforts have been made to review and classify ESMs, aiming to identify challenges and propose development pathways. In particular, Lopion et al. [10] and Ringkjøb et al. [11] classified ESMs according to the analytical approach, the assessed time horizon, the spatiotemporal resolution, the included technological and economic features, and the tool licensing. Prina et al. introduced the additional criteria of sectorial coverage and techno-economic resolution, which refers to the capability to model operation and flexibility features such as start-ups, shut-downs, ramps, and reserve of dispatchable units, as wells as self-discharge losses of storage systems [12]. Subsequently, Fodstad et al. considered also the methods to model uncertainty and social and human issues [13].

Energy system models are categorized into top-down and bottom-up models, depending on the adopted analytical approach. Top-down ESMs prioritise economic aspects while neglecting the complex set of interconnections of energy systems, and are therefore unable to address sector integration [10]. On the other hand, bottom-up models are based on a detailed implementation of the energy system components, whereas the impact on the economy is not considered. Considering such aspects, the remainder of the discussion will address only bottom-up models, since, from an engineering perspective, they are able to better represent the complexity of the decarbonisation problem [12]. Specifically, a pool of nearly 50 bottom-up ESMs (including variations and evolutions of the same models) is classified and discussed according to criteria regarding the mathematical approach, the spatial and temporal resolution, the considered time horizon, the included energy vectors and transport networks, and the covered end-use sectors. Models that focus solely on the power sector are excluded from the analysis, as cross-sectorial integration is essential to achieve complete decarbonisation.

A first distinction for ESMs regards the adopted mathematical method (see Table 1). Optimisation models are the most common option, as they enable the identification of the least-cost configuration of

Table 1
Energy system models review: method, spatial resolution, time resolution, and time scale.

Name	Method	Spatial resolution	Temporal resolution	Time horizon	Ref.
Balmorel	Opt.	Multi-node	Time slices	Evolutionary	[31–33]
Balmorel + OptiFlow	Opt.	Multi-node	Time slices	Snapshot	[34]
Calliope	Opt.	Multi-node	2-hour	Snapshot	[26,28]
DynEMo	Sim.	Single-node	Hourly	Evolutionary	[35]
EMPIRE	Opt.	Multi-node	Hourly	Evolutionary	[36]
EnergyPLAN	Sim.	Single-node	Hourly	Snapshot	[20,37,38]
Battaglia et al. (EnergyPLAN)	Sim.	Single-node	Hourly	Snapshot	[39]
Bellocchi et al. (EnergyPLAN)	Sim./Opt.	Single-node	Hourly	Snapshot	[40–42]
EnergyScope TD	Opt.	Multi-node	Typical days	Snapshot	[43,44]
Enertile	Opt.	Multi-node	Hourly	Evolutionary	[45,46]
EOLES_mv	Opt.	Single-node	Hourly	Snapshot	[47]
EPLANopt	Multi-obj.	Single-node	Hourly	Snapshot	[17]
EPLANoptMAC	Opt.	Single-node	Hourly	Snapshot	[48]
EPLANoptTP	Multi-obj.	Single-node	Hourly	Evolutionary	[18]
ESME	Opt.	Multi-node	Time slices	Evolutionary	[49]
FINE	Opt.	Multi-node	Hourly	Snapshot	[50]
GENESYS	Dispatch	Multi-node	Hourly	5 years	[14]
GENeSYS-MOD	Opt.	Multi-node	Time slices	Evolutionary	[51,52]
GRIMSEL-FLEX	Opt.	Multi-node	Hourly	Evolutionary	[53]
H2RES	Opt.	Single-node	Hourly	Evolutionary	[54]
I-ELGAS	Dispatch	Multi-node	Hourly	Snapshot	[16]
JRC-EU-TIMES	Opt.	Multi-node	Time slices	Evolutionary	[27]
LEAP	Sim.	Single-node	Annual	Evolutionary	[55–57]
LUT Energy System Transition Model	Opt.	Multi-node	Hourly	Evolutionary	[58,59]
MESSAGE	Opt.	Multi-node	Flexible	Evolutionary	[60]
METIS	Opt.	Multi-node	Hourly	Rolling horizon	[61]
NEMeSI (oemof)	Dispatch	Multi-node	Hourly	Snapshot	[15,62–64]
NEMO	Opt.	Multi-node	Time slices	Evolutionary	[65]
OCGModel (OSeMOSYS)	Opt.	Single-node	Time slices	Evolutionary	[66]
oemof	Opt.	Single-node	Hourly	Snapshot	[67,68]
oemof-moea	Multi-obj.	Multi-node	Hourly	Snapshot	[19]
OSeEMDE	Opt.	Multi-node	Hourly	Snapshot	[69]
OSeMBE	Opt.	Multi-node	Time slices	Evolutionary	[70]
OSeMOSYS	Opt.	Multi-node	Time slices	Evolutionary	[71,72]
PLEXOS	Opt.	Multi-node	Hourly	Snapshot	[73]
POLES	Sim.	Multi-node	Annual	Evolutionary	[74]
PRIMES	Opt.	Multi-node	5-year	Evolutionary	[75]
PyPSA	Opt.	Multi-node	Hourly	Evolutionary	[23]
PyPSA-Eur-Sec-30	Opt./MGA	Multi-node	Hourly	Snapshot	[76,77]
PyPSA-Eur-Sec	Opt.	Multi-node	3-hour	Snapshot/evolutionary	[29,30]
REMIND	Opt.	Multi-node	5-year or 10-year	Evolutionary	[78]
REMix	Opt.	Multi-node	Hourly	Evolutionary	[79–81]
REMod-D	Opt.	Single-node	Hourly	Evolutionary	[82–84]
Sector-coupled Euro-Calliope	MGA	Multi-node	2-hour	Snapshot	[25]
Temoa	Opt./MGA	Single-node	Time slices	Evolutionary	[22,85]
urbs	Opt.	Multi-node	Hourly	Snapshot	[86]
WEM	Sim.	Multi-node	Time slices	Snapshot	[87]
Colbertaldo et al. (Italy-P2G)	Sim.	Multi-node	Hourly	Snapshot	[88]
Colbertaldo et al. (California)	Opt.	Single-node	Hourly	Snapshot	[89]
Colbertaldo et al. (Italy-mobility)	Opt.	Multi-node	Hourly	Snapshot	[24]
Colbertaldo et al. (Italy-CCGT)	Opt.	Multi-node	Hourly	Snapshot	[90]
OMNI-ES (this work)	**Opt.**	**Multi-node**	**Hourly**	**Snapshot**	

the energy system. Since an essential characteristic of ESMs is to determine the required expansion of the installed capacity of all technologies, the objective function to be minimised includes both capital and operational expenditure. However, a subset of optimisation-based models considers only the energy vector dispatch, assigning capacities exogenously [14–16]. The existing literature features some examples of multi-objective optimisation models, which introduce the minimisation of CO_2 emissions as an additional objective function [17–19]. While the Pareto fronts obtained with such tools provide valuable insights on the trade-offs between cost optimality and emission reduction, the introduction of the second objective might be redundant considering that carbon neutrality is an imperative target in most recent policies. The second major category is that of simulation models, which are typically used to test and compare various system configurations. While this approach prevents the possibility to optimise the system performance, it has the advantage of a lower computational complexity, and, therefore, of shorter computational time. A simulation model is EnergyPLAN [20], which has been used in more than 70 publications and applied to analyse the energy system of numerous countries [21]. Modelling to Generate Alternatives (MGA) is a further approach, aimed at providing policy makers with a set of alternative near-optimal solutions rather than a unique optimal configuration. DeCarolis et al. developed the first example of MGA-based ESM, introducing this approach in the model Temoa [22].

Based on the adopted spatial resolution, ESMs can be divided into single-node and multi-node models (see Table 1). The former neglect the transport of energy vectors, together with the related bottlenecks and losses, thus assuming ideal transmission systems. This simplified approach has a limited impact when covering restricted geographical areas, whereas it may lead to significant inaccuracies when applied at the country or continent scale, especially in the case of areas characterised by uneven distribution of resources [12]. On the other hand, a multi-node approach enables the tracking of energy vector flows, and thus the identification of the infrastructural needs required to support the decarbonisation. Multi-node models are characterised by different spatial subdivisions depending on the model geographical coverage. For

example, nodes can correspond to countries [23], bidding zones of the electricity market [24,25], or regional administrative units [26].

Depending on the selected time horizon, ESMs are divided into snapshot or evolutionary models. Snapshot models typically analyse a single year, often referring to the target year of decarbonisation policies (e.g., 2030 or 2050). Evolutionary ESMs, instead, consider a longer time horizon, endogenously modelling the entire transition.

A fine temporal resolution is essential to capture the variability of intermittent renewable energy sources and the corresponding dynamics of the energy system in terms of storage and flexibility options. However, temporal resolution strongly impacts the computational performance, requiring modellers to find a trade-off between accuracy and computational time. As indicated in Table 1, a frequently adopted approach is to represent the year using a limited number of typical days or time slices. For example, the JRC-EU-TIMES model considers 12 time slices, which are representative of an average day, an average night, and a peak demand for each season of the year [27]. The accuracy can be improved by increasing the number of time steps employed to model the year. For example, the Calliope model adopts a 4-hour [26] or 2-hour resolution [25,28], and the most recent applications of PyPSA-Eur-Sec consider a 3-hour resolution [29,30]. The highest level of accuracy, instead, can be achieved (compatibly with the available data time series) by employing an hourly resolution, which yields a total of 8760 time steps per year [12].

Table 2 shows the ESMs classification according to the considered energy vectors and related transport networks. Given the planned phase-out of coal, the energy vectors that are expected to underpin future energy systems are electricity (EE), methane (CH_4, including fossil natural gas, synthetic and biogenic methane), hydrogen (H_2), and liquid fuels (LF, including oil-based, hydrogen-based, and biogenic fuels). Electricity is included in all ESMs, since most of them were originally developed to investigate the evolution of the power sector alone.

Table 2
Energy system models review: energy vectors and transport networks included in the model.

Name	Energy vectors				Transport networks				Ref.
	EE	CH_4	H_2	LF	EE	CH_4	H_2	LF	
Balmorel	✓	✓	✓		✓				[31–33]
Balmorel + OptiFlow	✓	✓	✓	✓	✓				[34]
Calliope	✓	✓	✓	✓	✓	✓			[26,28]
DynEMo	✓	✓	✓	✓					[35]
EMPIRE	✓				✓				[36]
EnergyPLAN	✓	✓	✓	✓					[20,37,38]
Battaglia et al. (EnergyPLAN)	✓	✓		✓					[39]
Bellocchi et al. (EnergyPLAN)	✓	✓	✓	✓					[40–42]
EnergyScope TD	✓	✓	✓	✓	✓				[43,44]
Enertile	✓	✓	✓		✓	✓			[45,46]
EOLES_mv	✓	✓	✓						[47]
EPLANopt	✓	✓	✓	✓					[17]
EPLANoptMAC	✓	✓	✓	✓					[48]
EPLANoptTP	✓			✓					[18]
ESME	✓	✓	✓	✓	✓		✓		[49]
FINE	✓		✓		✓		✓		[50]
GENESYS	✓		✓		✓				[14]
GENeSYS-MOD	✓	✓	✓	✓	✓				[51,52]
GRIMSEL-FLEX	✓				✓				[53]
H2RES	✓	✓	✓	✓					[54]
I-ELGAS	✓	✓	✓		✓	✓	✓		[16]
JRC-EU-TIMES	✓	✓	✓	✓	✓	✓	✓	✓	[27]
LEAP	✓	✓	✓	✓					[55–57]
LUT Energy System Transition Model	✓	✓	✓	✓	✓				[58,59]
MESSAGE	✓	✓	✓	✓	✓	✓		✓	[60]
METIS	✓	✓			✓	✓			[61]
NEMeSI (oemof)	✓	✓	✓	✓	✓				[15,62–64]
NEMO	✓	✓	✓	✓	✓				[65]
OCGModel (OSeMOSYS)	✓	✓		✓					[66]
oemof	✓								[67,68]
oemof-moea	✓	✓		✓	✓				[19]
OSeEMDE	✓		✓		✓		✓		[69]
OSeMBE	✓	✓		✓	✓				[70]
OSeMOSYS	✓	✓	✓	✓	✓				[71,72]
PLEXOS	✓	✓			✓	✓			[73]
POLES	✓	✓	✓	✓	✓	✓	✓	✓	[74]
PRIMES	✓	✓	✓	✓	✓	✓	✓		[75]
PyPSA	✓	✓	✓		✓				[23]
PyPSA-Eur-Sec-30	✓	✓	✓		✓				[76,77]
PyPSA-Eur-Sec	✓	✓	✓	✓	✓		✓		[29,30]
REMIND	✓	✓	✓	✓					[78]
REMix	✓	✓	✓		✓	✓	✓		[79–81]
REMod-D	✓	✓	✓	✓					[82–84]
Sector-coupled Euro-Calliope	✓	✓	✓	✓	✓				[25]
Temoa	✓	✓	✓	✓					[22,85]
urbs	✓	✓			✓	✓			[86]
WEM	✓	✓	✓	✓	✓	✓	✓	✓	[87]
Colbertaldo et al. (Italy-P2G)	✓	✓	✓		✓				[88]
Colbertaldo et al. (California)	✓		✓		✓				[89]
Colbertaldo et al. (Italy-mobility)	✓		✓		✓		✓		[24]
Colbertaldo et al. (Italy-CCGT)	✓	✓	✓		✓	✓			[90]
OMNI-ES (this work)	✓	✓	✓	✓	✓	✓	✓	✓	

Methane and hydrogen are also taken into account in most studies. However, they are generally considered only in intra-node conversion processes or as aggregated national demands, whereas their networks are neglected (e.g., Refs. [59,76]). Such an assumption introduces the approximation of excluding the transport of two fundamental carriers and makes ESMs unable to determine the required infrastructural developments and the related economic impact. In addition, in the case that hydrogen and synthetic fuels are considered, this approach assigns the entire burden of energy carrier transport to the electric grid, whereas the synergetic use of other infrastructures might lead to an improved system configuration. While different models permit to introduce multiple energy vector networks (e.g., Calliope [91], oemof [92], OSeMOSYS [71], PyPSA [77]), the existing literature features few examples of model applications. Also, the plurality of grids is often accompanied by simplifications to limit the computational complexity, such as the adoption of a coarser time resolution (e.g., Refs. [28,30,75,87]) or the waiver of complete optimisation [16]. Among hourly-resolved optimisation models, the CH_4 and H_2 networks are considered only in the REMix model [81], whereas Pickering et al. [25] represented fuel distribution by aggregating regional demands into an overall European demand, to which any region can contribute. A limited number of studies includes liquid fuels, and few of these consider carbon–neutral alternatives (e.g., Refs. [25,29,42,59]), frequently neglecting the transport network. This trend is determined by multiple factors. First, the sectors in which green liquid fuels might have a key role coincide with those that are more frequently neglected, such as aviation, navigation, or industrial feedstocks. As a result, many studies consider liquid fuels only as a residual presence of fossil fuels in road transport, considering its major evolution towards electric drivetrains. In addition, liquid fuels currently rely on a well-established supply chain, and their carbon–neutral alternatives do not require the development of a new infrastructure. Accordingly, ESMs typically prioritise the investigation of the transport networks of other energy vectors.

Energy system models can be categorised based on the included demand sectors and on the energy vectors that are considered in each sector (see Table 3). Although this criterion is significantly case-specific

Table 3
Energy system models review: energy vectors considered in demand sectors.

Name	Residential and services	Industry	Road transport	Aviation	Navigation	Ref.
Balmorel	EE, heat	EE, heat	EE	EE for LF	EE for LF	[31–33]
Balmorel + OptiFlow	EE, heat	EE, CH_4, heat	EE, H_2, LF	LF	LF	[34]
Calliope	EE	EE	EE			[26,28]
DynEMo	EE, heat	EE, CH_4, LF, heat	EE, LF	LF	LF	[35]
EMPIRE	EE	EE	EE			[36]
EnergyPLAN	EE, heat	EE, CH_4, heat	EE, H_2, LF	EE, H_2, LF	EE, H_2, LF	[20,37,38]
Battaglia et al. (EnergyPLAN)	EE, heat	EE, CH_4, LF, heat	EE, CH_4, LF			[39]
Bellocchi et al. (EnergyPLAN)	EE, heat	EE, CH_4, heat	EE, LF			[40–42]
EnergyScope TD	EE, heat	EE, heat	EE, H_2, LF			[43,44]
Enertile	EE, heat	EE, H_2, heat	EE, H_2			[45,46]
EOLES_mv	EE, heat	EE, heat	EE, CH_4			[47]
EPLANopt	EE, heat	EE, heat	EE, LF			[17]
EPLANoptMAC	EE, heat	EE, heat	EE, LF			[48]
EPLANoptTP	EE, heat	EE, heat	EE, LF			[18]
ESME	EE, heat	EE, H_2, CH_4, LF	EE, H_2, CH_4, LF			[49]
FINE	EE	EE	H_2			[50]
GENESYS	EE	EE				[14]
GENeSYS-MOD	EE, heat	EE, heat	EE, H_2, LF		LF	[51,52]
GRIMSEL-FLEX	EE, heat	EE				[53]
H2RES	EE, heat	EE, H_2, CH_4, LF	EE, H_2, LF			[54]
I-ELGAS	EE, CH_4, H_2	EE, CH_4, H_2	EE			[16]
JRC-EU-TIMES	EE, CH_4, H_2	EE, CH_4, LF, H_2	EE, LF, H_2	LF	LF	[27]
LEAP	User defined					[55–57]
LUT Energy System Transition Model	EE, heat	EE, heat, H_2, LF	EE, H_2, LF	EE, H_2, LF	EE, CH_4, LF	[58,59]
MESSAGE	EE, heat	EE, heat, CH_4, LF	EE, CH_4, H_2, LF	EE, LF	CH_4, H_2, LF	[60]
METIS	EE, CH_4	EE, CH_4	EE			[61]
NEMeSI (oemof)	EE, heat, H_2, LF (sectors not specified)					[15,62–64]
NEMO	EE	EE	EE			[65]
OCGModel (OSeMOSYS)	EE, heat	EE, heat	EE, LF	LF	LF	[66]
oemof	EE	EE	EE		EE	[67,68]
oemof-moea	EE, heat	EE, heat	EE, LF			[19]
OSeEMDE	EE, heat	EE				[69]
OSeMBE	EE	EE				[70]
OSeMOSYS	EE	EE	EE, LF			[71,72]
PLEXOS	EE, CH_4	EE, CH_4	EE, CH_4			[73]
POLES	EE, CH_4, LF, H_2	EE, H_2, LF, CH_4	EE, H_2, LF, CH_4	LF	LF	[74]
PRIMES	EE, heat	EE, H_2, LF, CH_4	EE, H_2, LF, CH_4	LF	LF, CH_4	[75]
PyPSA	EE, heat	EE, heat	EE			[23]
PyPSA-Eur-Sec-30	EE, heat	EE	EE, H_2			[76,77]
PyPSA-Eur-Sec	EE, heat	EE, H_2, LF, CH_4	EE, H_2, LF	LF	H_2	[29,30]
REMIND	EE, CH_4, LF, H_2	EE, H_2, LF, CH_4	EE, H_2, LF, CH_4			[78]
REMix	EE, heat	EE, heat, H_2	EE, H_2			[79–81]
REMod-D	EE, heat	EE, heat	EE, CH_4, H_2, LF	LF	LF	[82–84]
Sector-coupled Euro-Calliope	EE	EE, CH_4, H_2, LF	EE	LF	LF	[25]
Temoa	EE	EE	EE, CH_4, H_2, LF			[22,85]
urbs	EE, heat					[86]
WEM	EE, CH_4, LF, H_2	EE, H_2, LF, CH_4	EE, H_2, LF	LF	LF, CH_4	[87]
Colbertaldo et al. (Italy-P2G)	EE	EE	EE, H_2			[88]
Colbertaldo et al. (California)	EE	EE				[89]
Colbertaldo et al. (Italy-mobility)	EE	EE	EE, H_2			[24]
Colbertaldo et al. (Italy-CCGT)	EE, CH_4, H_2	EE, CH_4	EE, H_2			[90]
OMNI-ES (this work)	**EE, CH_4, H_2, LF**	**EE, CH_4, H_2, LF**	**EE, CH_4, H_2, LF**	**EE, H_2, LF**	**EE, H_2, LF**	

and the definition of sectors may vary depending on the study, it serves as a proxy of the extent to which ESMs are able to capture sector integration. In addition, all energy-consuming sectors must be included in order to account for all the possible CO_2 sources when addressing economy-wide carbon–neutral scenarios. A wide range of studies focus on the evolution of heating in the residential and services and industrial sectors, considering the competition between heat pumps and conventional boilers. Among them, some models directly consider heat as a separate demand sector (e.g., Refs. [17,58]), whereas others refer to the demand of energy vectors that are converted to heat (e.g., Refs. [16,25]). Only few exceptions do not take into account road transport, whereas aviation and navigation are often neglected, despite being among the major and hardest-to-decarbonise emitters. Electricity and heat demand of industry is included in most cases, often referring to historical demand or implementing simple projections of load increase. However, the evolution of the sector in terms of process heat electrification and green feedstocks is rarely addressed [25,29,59].

Despite the numerous efforts, the existing literature lacks a comprehensive approach that assesses the combined presence of multiple intertwined sectors, energy vectors, and networks, with a sufficiently refined spatiotemporal resolution. A truly holistic approach is required to address the decarbonisation problem, since the tools designed to outline the pathways towards net-zero CO_2 emissions must consider all the energy consuming sectors and all the possible solutions in order to be able to identify the optimal system configuration, taking into account the challenges and the advantages of the integration options.

1.2. Contribution of this work

This work aims to fill the identified research gaps by developing a linear programming (LP) bottom-up model that can determine the optimal configuration of the energy system at a country scale, covering all the demand sectors (residential and services, industry, road, air, and water transport) and considering a multiplicity of energy vectors (electricity, methane, hydrogen, liquid fuels – fossil, biogenic, or hydrogen-based), together with the related transport networks. This is obtained in the OMNI-ES model (Optimisation Model for Network-Integrated Energy Systems). The model is based on a multi-node formulation with a regional (NUTS-2) resolution and considers the hourly balances of energy vector over a year-long time frame with a perfect-foresight approach. It tracks the CO_2 flows in the system considering carbon sources, sinks, and usages, in order to introduce a net-zero emissions constraint.

This work leverages previous expertise on energy system modelling [24,88–90], which focused on the development of tools to address the evolution of the power and transport sectors. Here, the modelling approach enlarges the scope to the entire integrated energy system and looks at full decarbonisation over all sectors. The OMNI-ES model encompasses the whole complex set of interactions between sectors and energy vectors, in order to assess carbon–neutral scenarios. Compared to the existing literature (see Table 1-Table 3), the main novel aspect is the capability to simultaneously feature:

- an optimization-based approach that considers both the design and operation of the energy system;
- a high-resolution multi-node formulation;
- an hourly temporal resolution;
- a multi-vector structure that encompasses electricity, methane, hydrogen, and liquid fuels, considering both fossil and biogenic origins and the possibility to blend methane and hydrogen;
- the implementation of the transport networks of all the included energy vectors, also envisaging the possibility to use the existing gas infrastructure to deliver decarbonised carrier and the development of a new hydrogen supply chain;
- a comprehensive cross-sectorial approach, taking into account the evolution towards carbon-free options of all sectors;
- the introduction of a net-zero emission constraint through the direct and indirect CO_2 tracking, considering fossil fuel use, supply chains, unavoidable emissions, carbon capture and sequestration (CCS), direct air capture (DAC), natural absorption, and CO_2 use for P2L.

The scope of this work is to present the development of the OMNI-ES model, focusing on the formulated methodological approach, model structure, and analytical framework. As a model application, the case study of Italy is considered. Specifically, the analysis aims to assess the optimal energy system configuration that complies with the objective of carbon neutrality, considering 2050 as target year. The Italian decarbonisation pathway is an extremely interesting case study, considering that the country is required to switch from today's heavy reliance on foreign fossil fuel imports to a diametrically opposite exploitation of domestic renewable sources. In addition, Italy features a pronounced geographical mismatch between energy demand (concentrated in northern regions) and availability of renewable sources (more abundant in southern regions), yielding challenging infrastructural needs for transport and storage of energy vectors.

In this article, the model application serves the purpose of demonstrating the capabilities and potential of OMNI-ES. Accordingly, this work lays the foundations for subsequent analyses aiming at broadening the comparison of scenarios and developing policy-oriented assessments of the Italian case study, which will be addressed in upcoming works.

The remainder of the article is structured as follows. Section 2 provides a detailed description of the OMNI-ES model, in terms of framework, structure, and formulation. Then, Section 3 introduces the Italian scenario that is implemented in the case study, whereas Sections 4 and 5 discuss the results and the sensitivity analyses on some major assumptions. Thus, an overview of the model capabilities and potential are offered. Finally, Section 6 summarises the main conclusions and the most relevant understandings.

2. Methods

OMNI-ES is a bottom-up model able to investigate cost-optimal long-term scenarios under CO_2 emission constraints at a country scale, with a snapshot approach, i.e., studying a single target year. The tool is based on linear programming (LP) and is implemented in Matlab® with the aid of the YALMIP libraries [93], while the obtained optimisation problem can be solved with any commercial solver (such as Gurobi™ [94] or CPLEX™ [95]). Model results provide the optimal configuration and operation of the multi-sector integrated energy system in terms of installed capacities, domestic and imported energy resources exploitation, and flows of energy vectors and CO_2. The complete list of symbols used in equations is detailed in the Nomenclature Section. All exogenous parameters are distinguished using a tilde (~).

2.1. Model framework

The mathematical structure of OMNI-ES is schematised in Fig. 1. The combined presence of multiple energy vectors $v \in V$ is at the basis of the model formulation. These operate on parallel networks consisting of a set of nodes $n \in N$, which are connected to each other according to an assigned topology. As Fig. 1 shows, while the set of nodes N is unique, the network topologies differ for each energy vector, as nodes are connected through diverse pathways. A generic energy vector v enters a node of the related network through a set of sources $s \in S_v$, while end-use sectors $k \in K$ act as sinks. Note that, as the figure shows, the demand of a sector may involve multiple energy vectors. Nodes host the connection between networks through conversion processes $p \in P$. A single process may endogenously sink and/or source multiple energy vectors according to one or more conversion factors $\tilde{\alpha}_{p,v\to v'}$, thus

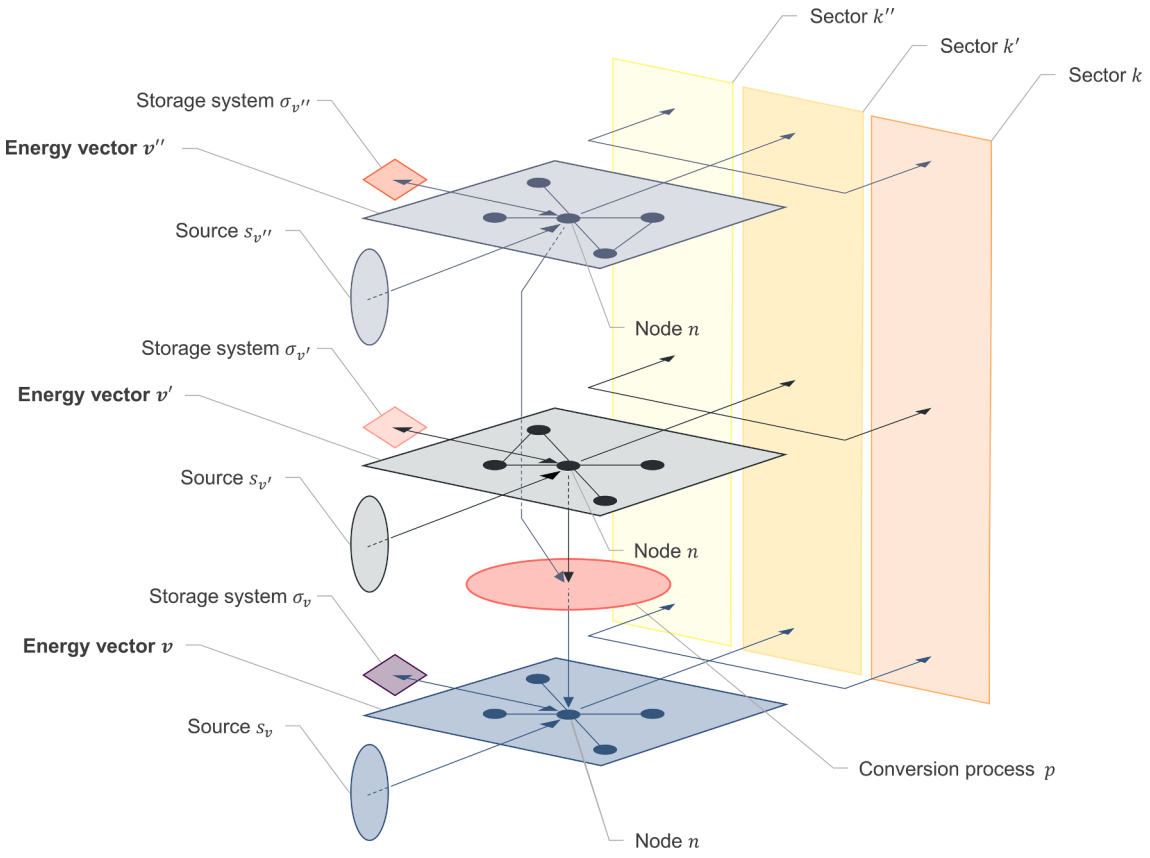

Fig. 1. Schematic representation of the mathematical structure of OMNI-ES.

connecting different networks. As an example, Fig. 1 shows a process that converts the energy vectors v' and v'' into energy vector v. Storage systems $\sigma_v \in \Sigma_v$ can be exploited to balance possible mismatches between generation and consumption. OMNI-ES enables the introduction of multiple storage technologies for each energy vector.

Figure 1 depicts the interaction among the described mathematical objects in a schematised manner. For the sake of readability, the figure displays, as an example, only one source and storage system for each energy vector, one conversion process with a single combination of energy vector flows, and a limited number of networks, nodes, and end-use sectors.

For each of the included energy vectors v, the model solves a balance equation to ensure the supply–demand match at each network node n and time step t. Considering the mathematical structure schematised in Fig. 1, the balance equation is:

$$\forall v,n,t \quad \sum_{s\in S_v} q^{n,t}_{s,v} + \sum_{p\in P} q^{n,t}_{\mathrm{otp},p,v} + \sum_{\sigma_v\in\Sigma_v} q^{n,t}_{\mathrm{otp},\sigma_v,v} + \sum_{n'\in N} q^{n,n',t}_{\mathrm{trn},v} = \sum_{k\in K} \tilde{q}^{n,t}_{\mathrm{dem},k,v} + \sum_{p\in P} q^{n,t}_{\mathrm{ipt},p,v} + \sum_{\sigma_v\in\Sigma_v} q^{n,t}_{\mathrm{ipt},\sigma_v,v} + q^{n,t}_{\mathrm{crt},v} \tag{1}$$

where quantities are expressed in terms of energy content, i.e., in MWh per unit of time. Given the hourly resolution, this is equivalent to the average power in the time step.

Typically, multiple sources $q^{n,t}_{s,v}$ are available for a single energy vector, as these can be either fossil or renewable, as well as domestic or imported from abroad. Conversion processes endogenously introduce both source ($q^{n,t}_{\mathrm{otp},p,v}$) and sink ($q^{n,t}_{\mathrm{ipt},p,v}$) terms. These couple the different balance equations, as the input and output flows of a process relates multiple energy vectors through the conversion factors $\tilde{\alpha}_{p,v'\to v}$, as expressed in Eq. (2). Energy vector transport is accounted for in the variable $q^{n,n',t}_{\mathrm{trn},v}$, which represents the quantity exchanged between n and a neighbouring node n', assuming the flow positive if entering node n. Connections among nodes are determined by the network topology, and thus may differ depending on the energy vector. The term $\tilde{q}^{n,t}_{\mathrm{dem},k,v}$ represents the exogenous demand of the end-use sector k, while the possibility of curtailment is included with the quantity $q^{n,t}_{\mathrm{crt},v}$. Multiple storage technologies may be available for a single energy vector, and the variables $q^{n,t}_{\mathrm{ipt},\sigma_v,v}$ and $q^{n,t}_{\mathrm{otp},\sigma_v,v}$ represent the input and output storage flow, respectively. These terms are used to track the time evolution of the storage content ($Q^{n,t}_{\sigma_v,v}$) as reported in Eq. (3), where $\tilde{\Delta}t$ represents the temporal resolution of the model, $\tilde{\eta}_{\mathrm{ipt},\sigma_v}$ and $\tilde{\eta}_{\mathrm{otp},\sigma_v}$ are the charge and discharge efficiencies, and $\tilde{\varepsilon}_{\sigma_v,v}$ is the self-discharge coefficient specific to the duration of the time step. In order to ensure the cyclic operation of the system, the storage content at the end of the time horizon ($Q^{n,t_{end}}_{\sigma_v,v}$) is constrained to be equal or larger than the initial quantity ($Q^{n,t_{start}}_{\sigma_v,v}$), as shown in Eq. (4).

$$\forall v,p,n,t \quad q^{n,t}_{\mathrm{otp},p,v} = \sum_{v'\in V} q^{n,t}_{\mathrm{ipt},p,v'} \tilde{\alpha}_{p,v'\to v} \tag{2}$$

$$\forall v,\sigma_v,n,t \quad Q^{n,t+1}_{\sigma_v,v} = Q^{n,t}_{\sigma_v,v}\left(1-\tilde{\varepsilon}_{\sigma_v,v}\right) + q^{n,t}_{ipt,\sigma_v,v}\tilde{\Delta t}\,\tilde{\eta}_{ipt,\sigma_v,v} - \frac{q^{n,t}_{otp,\sigma_v,v}\tilde{\Delta t}}{\tilde{\eta}_{otp,\sigma_v,v}} \tag{3}$$

$$\forall v,\sigma_v,n \quad Q^{n,t_{end}}_{\sigma_v,v} \geq Q^{n,t_{start}}_{\sigma_v,v} \tag{4}$$

For each of the included technology $i \in I$, flows are constrained by the installed capacity (Eq. (5)), which is a decision variable and contributes to the capital expenditures. In turn, the installed capacity may be bounded by an exogeneous limit (Eq. (6)). The exploitation of sources is exogenously limited within the available potential (Eq. (7)), according to the boundary conditions of the analysed scenario. In some cases, such

as biomass, the source may feed more than one network. In this case, there is a competition between sectors, and the availability must account for all destinations.

$$\forall v, i, n, t \quad q_{i,v}^{n,t} \leq C_i^n \tag{5}$$

$$\forall i, n \quad C_i^n \leq \tilde{C}_{i,UB}^{n} \tag{6}$$

$$\forall s, n \quad \sum_{t\in T}\sum_{v\in V} q_{s,v}^{n,t} \leq \tilde{C}_{s,UB}^{n} \tag{7}$$

In Section 2.3, the presented formulation will be declined for the balances of electricity, gas, hydrogen, liquid fuel, and CO_2.

2.2. Model structure

The presented mathematical structure is implemented to model the energy vector and CO_2 flows as schematised in Fig. 2. The model is developed adopting a technology-neutral approach, including all the relevant energy vectors and the related conversion and storage technologies. Specifically, electricity (EE), gas (G), hydrogen (H_2), and liquid fuels (LF) are the considered energy vectors. Methane accounts for both fossil natural gas and biomethane, and the blending with hydrogen in the existing gas infrastructure is enabled. In this way, the gas network always operates with a CH_4-H_2 blend, with variable fractions of methane (G-CH_4) and hydrogen (G-H_2). The model encompasses different types of liquid fuels (oil-based, biofuels, and e-fuels), which are assumed to have the same physical properties despite different production pathways, costs, and carbon footprint of the supply chains. The flows of CO_2 are tracked considering carbon sources (combustion of fossil fuels, emissions related to the supply chains of imported energy vectors), sinks (carbon capture and storage, direct air capture), and utilisations (conversion to e-fuels).

As depicted in Fig. 1, OMNI-ES relies on a multi-node and multi-network spatial resolution, since it is essential to account for transport losses and possible bottlenecks in the existing infrastructures (e.g., the electric and natural gas grids), as well as to identify the infrastructural needs that emerge with the deployment of new energy vectors (e.g., hydrogen). The adopted spatial resolution determines the cardinality of the set of nodes N (i.e., the number of nodes), while network topologies are specific to each energy vector. Edges represent aggregates of connections, which set the transfer limit in terms of energy flows that can be exchanged between adjacent nodes in each time step.

As far as the temporal resolution is concerned, the model adopts a snapshot approach, as the optimisation time horizon corresponds to a single target year. In order to fully capture the variability of intermittent renewable energy sources and to properly size storage systems, an hourly resolution is considered, yielding a total of 8760 time steps.

The model objective is the minimisation of the total annual cost, which includes the annualised capital expenses, variable and fixed operational costs. Capacity expansion is considered for all the included technologies adopting a brownfield approach, i.e., accounting for the capital expenses of additional installations only, assuming that the replacement of already-installed capacity would take place anyway.

2.3. Model formulation

This section outlines the analytical formulation of the model, presenting the objective function and the main variables and equations of the optimisation problem. According to the adopted LP approach, all the equations are required to be linear, and variables must take real values.

2.3.1. Objective function

The model objective is the minimisation of the total annual cost over the time horizon of the target year, assuming perfectly competitive markets. The total annual cost (TAC) includes all the capital and operational expenditures:

$$TAC = \sum_{i\in I} CAPEX_i \cdot \tilde{CRF}_i + \sum_{j\in J} OPEX_j \tag{8}$$

where $i \in I$ represents a generic technology of the energy system, $j \in J$ represents a generic operational expenditure item, and $\tilde{CRF}_i$ is the related capital recovery factor. The latter is required to annualise

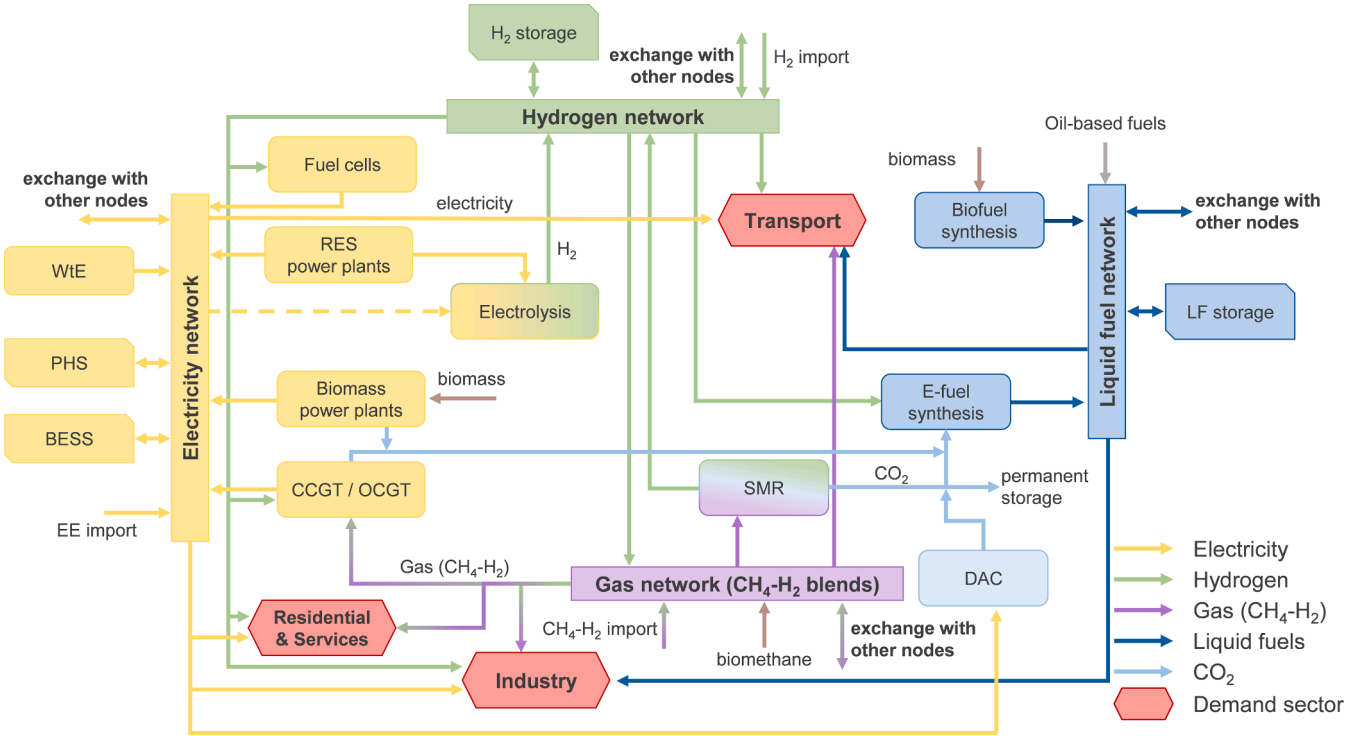

Fig. 2. Schematic representation of the energy vector and CO_2 flows within one node.

investments and is computed from lifetime (also dependent upon the technology) and the discount factor (assumed unique for all technologies).

OMNI-ES adopts a brownfield approach, assuming that the installed capacities of most relevant technologies (e.g., solar and wind power generation) will be replaced anyway at the end of their lifetime and are therefore not additional. The capital expenditure of a technology is computed as the product of a specific investment cost and the difference between the additional capacity that is installed with respect to the reference, considering all network nodes:

$$CAPEX_i = \sum_{n \in N} \tilde{\text{capex}}_i \left(C_i^n - \tilde{C}_{i,ref}^n \right) \tag{9}$$

Operational expenditures include fixed (*FC*) and variable (*VC*) costs of the considered technologies, computed via Eqs. (10)-(15). Specifically, fixed expenditures account for operation and maintenance (O&M) and are mainly expressed as a percentage of capital costs ($\tilde{\text{opex}}_{\%\text{fix},i}$), while variable costs include the variable OPEX of the considered technologies ($OPEX_{\text{var}}$), the procurement of sources (VC_S), and the transport costs of all energy vectors (VC_{trn}). The latter represent the total annual expenditures incurred by transmission system operators (TSOs – assuming that one will exist for each energy vector), as the specific cost $\tilde{c}_{\text{trn},v}$ is an average cost that accounts for both capital and operational expenditures and is applied to the cumulative annual flows that are managed by each infrastructure.

$$\sum_{j \in J} OPEX_j = FC + VC \tag{10}$$

$$FC = \sum_{i \in I} \tilde{\text{opex}}_{\%\text{fix},i} CAPEX_i \tag{11}$$

$$VC = OPEX_{\text{var}} + VC_s + VC_{\text{trn}} \tag{12}$$

$$OPEX_{\text{var}} = \sum_{v \in V} \sum_{i \in I} \sum_{n \in N} \sum_{t \in T} \tilde{\text{opex}}_{\text{var},i,v}\, q_{i,v}^{n,t} \tag{13}$$

$$VC_S = \sum_{v \in V} \sum_{s \in S_v} \sum_{n \in N} \sum_{t \in T} \tilde{c}_{s,v}\, q_{s,v}^{n,t} \tag{14}$$

$$VC_{\text{trn}} = \sum_{v \in V} \sum_{n \in N} \sum_{t \in T} \tilde{c}_{\text{trn},v} \left(\sum_{s \in S_v} q_{s,v}^{n,t} + \sum_{p \in P} q_{\text{otp},p,v}^{n,t} \right) \tag{15}$$

2.3.2. Electricity

The electricity network includes power generation from renewable sources or waste as well as via fuel cells (FCs), combined-cycle gas turbines (CCGTs), and open-cycle gas turbines (OCGTs). Renewable sources are distinguished between non-dispatchable (solar photovoltaic, onshore wind, offshore wind, run-of-river hydro) for which a given output profile is provided and dispatchable (reservoir-based hydro, geothermal, biomass) whose output can regulate within the availability of the feed. Referring to the structure of Eq. (1), RES, biomass, and waste power plants are modelled as electricity sources since their input feed is not a vector of the model, whereas FCs, CCGTs, and OCGTs are described as conversion processes. Gas-fuelled plants are fed with a CH_4-H_2 blend, whose modelling approach is discussed in Section 2.3.3. Electricity import is enabled in nodes that correspond to grid connections to foreign countries and is modelled as a source in the balance equation. Regarding electric storage, battery energy storage systems (BESS) and pumped hydro storage (PHS) are the considered options, but more could be introduced with the same approach.

The electricity balance equation features various endogenous consumption terms, which are related to conversion processes that output other energy vectors. These include electrolysis, CO_2 capture, direct air capture (DAC), and hydrogen separation devices in the gas grid. Electricity conversion into hydrogen through electrolysis (P2H) unlocks an additional storage option, as it can be stored and later reconverted into electricity through FCs, CCGTs, and/or OCGTs.

The resulting nodal balance equation is:

$$\begin{aligned} \forall n,t \quad & q_{\text{pvt},EE}^{n,t} + q_{\text{wnn},EE}^{n,t} + q_{\text{wno},EE}^{n,t} + q_{\text{hyd},EE}^{n,t} + q_{\text{geo},EE}^{n,t} + q_{\text{bms},EE}^{n,t} + q_{\text{WtE},EE}^{n,t} \\ & + q_{\text{imp},EE}^{n,t} + q_{\text{otp},fcs,EE}^{n,t} + q_{\text{otp},cgt,EE}^{n,t} + q_{\text{otp},ogt,EE}^{n,t} + q_{\text{otp},bes,EE}^{n,t} + q_{\text{otp},phs,EE}^{n,t} \\ & + \sum_{n' \in N} q_{\text{trn},EE}^{n,n',t} = \sum_{k \in K} \tilde{q}_{\text{dem},k,EE}^{n,t} + q_{\text{ipt},elc,EE}^{n,t} + q_{\text{ipt},cpt,EE}^{n,t} + q_{\text{ipt},dac,EE}^{n,t} \\ & + q_{\text{ipt},sep,EE}^{n,t} + q_{\text{ipt},bes,EE}^{n,t} + q_{\text{ipt},phs,EE}^{n,t} + q_{\text{crt},EE}^{n,t} \end{aligned} \tag{16}$$

2.3.3. Gas

The gas network is representative of the existing natural gas infrastructure, assuming that pipelines are upgraded to operate with a blend of CH_4 and H_2. Such a system is modelled by fictitiously splitting the network into a CH_4 grid and a H_2 grid, which are topologically identical to the existing natural gas network. This approach results in two balance equations (Eq. (17) for CH_4 and Eq. (18) for H_2), which are coupled through common consumption terms (Eqs. (19)-(21)) and transport capacity limits (Eq. (23)). The modelling approach is schematised in Fig. 3 considering the interaction of the gas system with another energy vector v' through a generic production process and the demand of one sector.

Source terms in the CH_4 equation (Eq. (17)) include domestic and imported natural gas, which are distinguished in terms of supply chain-related emissions, and biomethane production via biogas upgrading. In the H_2 equation (Eq. (18)), the import of both green and blue hydrogen is considered at nodes with external connections, while the local injection of domestic hydrogen is enabled at each node. The exogenous demand of each sector (Eq. (19)) is defined in terms of gas energy content and can be covered by a blend with a variable hydrogen fraction, which is endogenously optimised within the assigned limits (Eq. (22)). The same holds for the endogenous gas consumption of CCGTs and OCGTs, which take an aggregated gas input ($q_{\text{ipt},cgt,G}^{n,t}$ and $q_{\text{ipt},ogt,G}^{n,t}$, computed through Eqs. (20)-(21)) and convert it into electricity ($q_{\text{otp},cgt,EE}^{n,t}$ and $q_{\text{otp},ogt,EE}^{n,t}$ in Eq. (16)). The allowed hydrogen fraction is set to zero for technologies that specifically require methane, such as natural gas-fuelled vehicles, methane-based steel production via direct reduction of iron ore (CH_4-DRI), and steam methane reforming (SMR). Hydrogen separation for pure uses is allowed, tracking the related electricity consumption ($q_{\text{ipt},sep,EE}^{n,t}$ in Eq. (16)). As Eq. (23) shows, the transported quantity is bounded by the size of the pipelines (assumed as the existing and the planned within the investigated time horizon), while the maximum hydrogen fraction might be exogenously constrained according to the gas grid regulation, which in turn depends on the level of pipeline reconversion (Eq. (24)).

The model does not detail gas storage but rather encompasses seasonal storage needs through the hydrogen infrastructure. Given the constrained availability of biomethane and the limited room for natural gas use in net-zero CO_2 emission scenarios, methane is expected to have a minor role, making the storage of variable CH_4-H_2 blend a rather complex and unappealing option. In addition, clean hydrogen production necessarily requires storage, while methane production is not subject to the availability of intermittent renewables. From a mathematical point of view, the implementation of a gas storage system treating a variable blend would introduce significant modelling complexity, introducing possible non-linearities and/or binary variables to preserve the gas composition in the output flows and to guarantee consistency of CH_4 and H_2 flows.

$$\begin{aligned} \forall n,t \quad & q_{\text{bmt},G\text{-}CH_4}^{n,t} + q_{\text{NGdom},G\text{-}CH_4}^{n,t} + q_{\text{impNG},G\text{-}CH_4}^{n,t} + \sum_{n' \in N} q_{\text{trn},G\text{-}CH_4}^{n,n',t} \\ & = q_{\text{dem},G\text{-}CH_4}^{n,t} + q_{\text{ipt},cgt,G\text{-}CH_4}^{n,t} + q_{\text{ipt},ogt,G\text{-}CH_4}^{n,t} + q_{\text{ipt},smr,G\text{-}CH_4}^{n,t} \end{aligned} \tag{17}$$

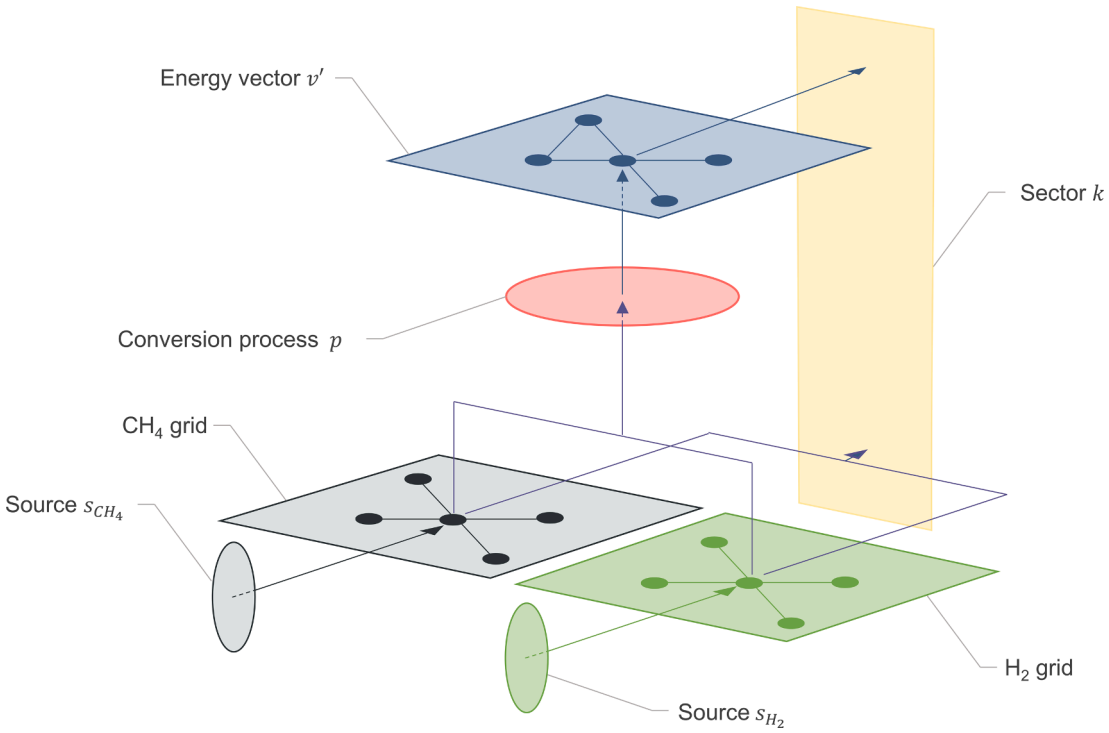

Fig. 3. Schematisation of the gas network modelling approach.

$$\forall n,t \quad q^{n,t}_{\text{impGRN},G\text{-}H_2} + q^{n,t}_{\text{impBLU},G\text{-}H_2} + q^{n,t}_{\text{otp},inj,G\text{-}H_2} + \sum_{n^{'}\in N} q^{n,n^{'},t}_{\text{trn},G\text{-}H_2} = q^{n,t}_{\text{dem},G\text{-}H_2} + q^{n,t}_{\text{ipt},cgt,G\text{-}H_2} + q^{n,t}_{\text{ipt},ogt,G\text{-}H_2} + q^{n,t}_{\text{ipt},sep,G\text{-}H_2} \tag{18}$$

$$\forall n,t,k \quad q^{n,t}_{\text{dem},G\text{-}H_2} + q^{n,t}_{\text{dem},G\text{-}CH_4} = \tilde{q}^{n,t}_{\text{dem},k,G} \tag{19}$$

$$\forall n,t \quad q^{n,t}_{\text{ipt},cgt,G\text{-}H_2} + q^{n,t}_{\text{ipt},cgt,G\text{-}CH_4} = q^{n,t}_{\text{ipt},cgt,G} \tag{20}$$

$$\forall n,t \quad q^{n,t}_{\text{ipt},ogt,G\text{-}H_2} + q^{n,t}_{\text{ipt},ogt,G\text{-}CH_4} = q^{n,t}_{\text{ipt},ogt,G} \tag{21}$$

$$\forall n,t,i \quad q^{n,t}_{i,G\text{-}H_2} \le \tilde{x}_{H_2,max,i} q^{n,t}_{i,G} \tag{22}$$

$$\forall n,t \quad q^{n,n^{'},t}_{\text{trn},G\text{-}H_2} \tilde{\nu}_{H_2} + q^{n,n^{'},t}_{\text{trn},G\text{-}CH_4} \tilde{\nu}_{CH_4} \le \tilde{C}^{n,n^{'}}_{\text{trn},G} \tag{23}$$

$$\forall n,t \quad q^{n,n^{'},t}_{\text{trn},G\text{-}H_2} \le \tilde{x}^{n,n^{'}}_{H_2,max,\text{trn}} \left(q^{n,n^{'},t}_{\text{trn},G\text{-}H_2} + q^{n,n^{'},t}_{\text{trn},G\text{-}CH_4} \right) \tag{24}$$

2.3.4. Hydrogen

The development of a dedicated hydrogen delivery network is required to enable the deployment of such energy vector when the gas infrastructure is not suitable, e.g., due to saturated transport capacity and/or reached limit on the hydrogen fraction in the CH_4-H_2 blend.

The nodal balance equation of the hydrogen network is:

$$\forall n,t \quad q^{n,t}_{\text{impGRN},H_2} + q^{n,t}_{\text{impBLU},H_2} + q^{n,t}_{\text{otp},elc,H_2} + q^{n,t}_{\text{otp},smr,H_2} + q^{n,t}_{\text{otp},sep,H_2} + \sum_{\sigma_{H_2}\in\Sigma_{H_2}} q^{n,t}_{\text{otp},\sigma_{H_2},H_2} + \sum_{n^{'}\in N} q^{n,n^{'},t}_{\text{trn},H_2} = \sum_{k\in K} \tilde{q}^{n,t}_{\text{dem},k,H_2} + \sum_{\sigma_{H_2}\in\Sigma_{H_2}} q^{n,t}_{\text{ipt},\sigma_{H_2},H_2} + q^{n,t}_{\text{ipt},fcs,H_2} + q^{n,t}_{\text{ipt},inj,H_2} + q^{n,t}_{\text{ipt},EFp,H_2} \tag{25}$$

Hydrogen supply includes the import of green and blue hydrogen, the production via electrolysis and SMR, and the separation from gas (CH_4-H_2 blend), which is associated to an energetic cost in the electricity equation ($q^{n,t}_{\text{ipt},sep,EE}$ in Eq. (16)). Consumption terms involve uses that require pure hydrogen, such as the exogenous demand of some end-use applications (e.g., FCEVs, carbon-free ammonia production, etc.), the consumption of fuel cells and e-fuel production systems, and the injection in the gas grid. Hydrogen storage is a critical element of the energy systems and interacts with the hydrogen network via input/output flows, on which charge and discharge losses are applied. OMNI-ES is capable to include multiple technologies, each involving limits on minimum and maximum capacity and on input/output flow rates.

2.3.5. Liquid fuels

The model considers multiple types of liquid fuels, taking into account the different production processes, supply chains, and economic parameters. These include conventional oil-based fuels, biofuels, and hydrogen-based e-fuels. In the balance equation (Eq. (26)), imports are distinguished between oil-based ("grey") and carbon–neutral ("green") fuels, which are characterised by different costs and carbon content. Biofuel production ($q^{n,t}_{\text{otp},BFp,\text{LF}}$) is modelled considering that the related biomass consumption is constrained by a limited availability and competes with that of biomass-based power generation ($q^{n,t}_{\text{bms},EE}$ in Eq. (16)). The e-fuel production term involves the endogenous consumption of hydrogen and CO_2, thus coupling the related balance equations (Eq. (25) and (27)). After injection into a node, the different liquid fuel types are assumed to have the same physical properties, considering the transport and consumption of one aggregate fuel in a single network.

$$\forall n,t \quad q^{n,t}_{\text{impGRN},LF} + q^{n,t}_{\text{impGREY},LF} + q^{n,t}_{\text{otp},BFp,\text{LF}} + q^{n,t}_{\text{otp},EFp,LF} + q^{n,t}_{\text{otp},str,LF} + \sum_{n^{'}\in N} q^{n,n^{'},t}_{\text{trn},LF} = \sum_{k\in K} \tilde{q}^{n,t}_{\text{dem},k,LF} + q^{n,t}_{\text{ipt},str,LF} \tag{26}$$

2.3.6. CO_2 tracking

The CO_2 balance is tracked via Eq. (27), accounting for carbon sources, sinks, and uses. The balance is implemented on an annual basis, avoiding the need of modelling local storage of CO_2, which would be required to compensate temporal mismatches of CO_2 availability with respect to e-fuel production. Inter-nodal transport of CO_2 is neglected since it appears economically disadvantageous with respect to that of liquid fuels or hydrogen. In particular, the latter is expected to be

transported in any case, with significant hydrogen quantities exported from nodes with favourable production conditions, as the exogeneous demand of H_2 already introduces considerable quantities. Instead, long-distance transport of CO_2 is considered introducing an economic expenditure on the amount sent to permanent sequestration, without focusing on topologies. The detailed modelling of a CO_2 network comprising both inter-nodal and long-distance transport and tracking exchange flows is postponed to future model developments, where potential synergies and possible backbones will be studied.

$$\forall n \quad \sum_{t\in T}\left(\sum_{i\in I} q^{n,t}_{\mathrm{otp},cpt,i,CO_2} + q^{n,t}_{\mathrm{otp,dac},CO_2}\right) = \sum_{t\in T}\left(\sum_{k\in K} \tilde{q}^{n,t}_{dem,k,CO_2} + q^{n,t}_{\mathrm{ipt},EFp,CO_2} + q^{n,t}_{\mathrm{str},CO_2}\right) \tag{27}$$

The sources of CO_2 are capture from flue gases ($q^{n,t}_{\mathrm{otp},cpt,i,CO_2}$) and extraction from the atmosphere through DAC ($q^{n,t}_{\mathrm{otp},dac,CO_2}$). The former may be applied on conversion processes (e.g., thermoelectric power generation, steam methane reforming, biogas upgrading) and industrial processes (e.g., primary steelmaking and cement production), adopting either fossil or biogenic input. The available CO_2 can be used to satisfy an exogenous demand (e.g., for industrial methanol production), converted to produce e-fuels, or permanently stored.

The tracking of CO_2 flows enables the introduction of a net-zero-emission constraint, defined as:

$$\sum_{n\in N}\sum_{t\in T}\left[\left(q^{n,t}_{\mathrm{NGdom},G\text{-}CH_4} + q^{n,t}_{\mathrm{impNG},G\text{-}CH_4}\right)\tilde{e}_{CO_2,NG} + q^{n,t}_{\mathrm{impGREY},LF}\tilde{e}_{CO_2,LF} + \frac{q^{n,t}_{wst,EE}}{\tilde{\eta}_{WtE}}\tilde{e}_{CO_2 wst}\right] + q_{\mathrm{sc},CO_2} + \tilde{q}_{\mathrm{una},CO_2} - \tilde{q}_{\mathrm{abs},CO_2} - \sum_{n\in N}\sum_{t\in T} q^{n,t}_{\mathrm{str},CO_2} - q_{\mathrm{ext},CO_2} = 0 \tag{28}$$

The fossil CO_2 that enters the system boundaries derives from the carbon contained in natural gas, oil-based liquid fuels, and waste (all within the square brackets in the left-hand side of the equation), from supply chain-related emissions (q_{sc,CO_2}), and from unavoidable emissions that cannot be directly eliminated ($\tilde{q}_{\mathrm{una},CO_2}$). To satisfy the net-zero-emission constraint, these terms must be compensated through either natural absorption ($\tilde{q}_{\mathrm{abs},CO_2}$) or permanent storage ($q^{n,t}_{\mathrm{str},CO_2}$). The constraint equation also features the closure term q_{ext,CO_2}.

The implemented CO_2 balances guarantee that the CO_2 used in conversion processes within the energy system originate from domestic capture or DAC, while the compensation of unavoidable emissions and residual emissions from capture-equipped processes takes place via negative emissions (CO_2 capture on processes fed with carbon–neutral vectors) or via the closure term ('ext'). This 'extra' term represents very-high-cost compensation options, such as out-of-borders DAC units plus sequestration or forestation measures, and is not further detailed. In this way, OMNI-ES prioritises sequestration from CO_2 capture in conversion or industrial processes rather than from additional DAC-originated flows. Details on unavoidable emissions and natural absorption are available in Supplementary Material for the case study.

3. Scenario definition

The OMNI-ES model is here applied to investigate a long-term scenario for Italy. Specifically, the case study considers 2050 as target year, requiring the achievement of economy-wide decarbonisation. The main assumptions for the scenario definition are discussed in this section, focusing on the adopted methodological approach, whereas additional details and data sources are reported in Supplementary Material. For each of the included technologies, techno-economic data are selected according to projections and expected trends, considering the year 2050 as reference. The list of the employed input data is reported in Supplementary Material.

3.1. End-use sectors

OMNI-ES requires as input a series of exogenously defined energy vector demand quantities and profiles. The analysis considers the evolution of all end-use sectors (residential and services, transport, industry) towards the adoption of decarbonised options. Accordingly, the projected demand of energy vectors is determined, starting from the final demand (e.g., heat provided, km travelled, …), considering the switch to clean technologies of all economic activities, as detailed in the following sections. Fig. 4 shows the resulting energy vector demand by sector in Italy as it is exogenously assigned as input to OMNI-ES. The figure displays demand shares and total annual values, considering the conversion efficiencies of the different technologies to provide the final products or services. The total energy vector consumption of the scenario will be higher than the demand values reported in the figure, due to the additional contribution of endogenous consumptions in conversion processes.

The electric load is determined considering the projections of two terms: the conventional consumers demand, based on population and gross domestic product (GDP) growth, as well as increased electrification in households as assumed by the national transmission system operators [96], and the additional demand from the electrification of heating in the residential and services sector (see Section 3.1.1), transport (see Section 3.1.2), and process heat generation in industry (see Section 3.1.3). The hourly-resolved profiles of consumers demand of electricity are built based on historical time series by ENTSO-E [97]. The gas demand is assumed to be satisfied with a CH_4-H_2 blend with a hydrogen fraction up to 100%. This includes the projected consumers demand as defined by the TSO [96], excluding the contribution of heating, high-temperature process heat generation, and industrial feedstocks. The analysis assumes a considerable reduction of the gas consumption for heating in the residential and services sector, for which only a residual use of gas systems is considered (see Section 3.1.1). Besides the injection in the gas grid, direct hydrogen uses encompass applications in transport and industry. The use of liquid fuels is envisaged in the transport sector and in industry, considering the potential exploitation of carbon–neutral fuels (i.e., biofuels and e-fuels) in internal combustion engines, aviation, and navigation (see Section 3.1.2) and as chemical feedstocks (see Section 3.1.3). As discussed in Section 3.1.3, the chemical industry features an exogenous demand of CO_2 as feedstock, which is not shown in Fig. 4 since it cannot be represented on energy basis.

Both the electricity and gas consumers demands are regionalised according to historical data, considering the regional shares on the annual demand [98,99]. Based on data availability, hourly-resolved electricity demand profiles are assumed to have the same shape (i.e., the same normalised profile with respect to the total regional annual demand) in all regions within the same bidding zones. Regarding the consumers gas demand, the limited availability of data requires to assume that all regions feature the same demand profile shape. Assumptions for the regionalisation of sector-specific demand data are discussed in the related sections and detailed in Supplementary Material.

3.1.1. Heating and cooling

The heating demand in the residential and services sector is determined assuming a strong effort in building renovation and refurbishment, leading to a massive presence of electric heat pumps (HPs), which satisfy 75% of the thermal demand. The remainder of demand is covered by biomass-based heating, district heating, and gas systems fed by a

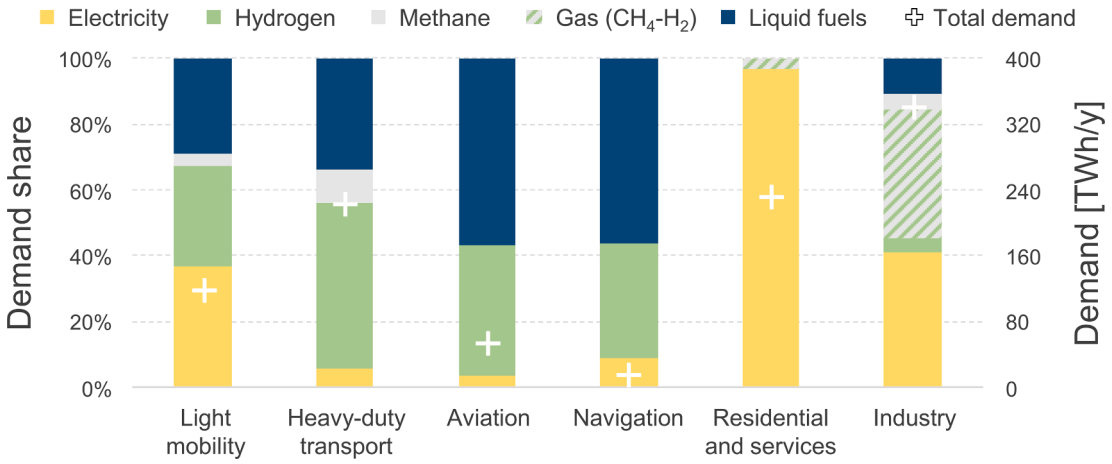

Fig. 4. Energy vector demand in the carbon neutral scenario for Italy: shares on energy basis (left) and total quantity (right axis). Light mobility includes passenger cars and light-duty vehicles.

CH_4-H_2 blend in non-refurbished buildings.

Hourly-resolved profiles for electricity and gas (CH_4-H_2 blend) consumptions are built following the methodology presented in Refs. [100–102]. In particular, the heating demand is estimated considering the different building categories, depending on construction age and thermal dispersions. Data are collected at municipality level, and then aggregated at regional scale. Electric heat pumps are assumed to be installed in refurbished buildings, considering the use of air-to-air heat pumps in municipalities with heating degree days (HDD) below 2000 and air-to-water heat pumps in municipalities with HDD above 2000. Hourly-resolved profiles are computed according to the variation of ambient temperatures for air-to-air HPs (considering 2019 as reference year) and using the bin method [102] for air-to-water HPs. For both systems, the variation of the coefficient of performance (COP) depending on ambient and supply temperatures is considered. Gas heating is assumed to be based on gas absorption heat pumps, and the related hourly-resolved consumption is determined according to the variation of ambient temperature (considering 2019 as reference year) and considering a variable gas utilisation efficiency depending on ambient and supply temperatures. The resulting exogenous demands of electricity and gas are 58 TWh_e/y and 8 TWh_{LHV}/y, respectively.

Biomass boilers are assumed to cover approximately 5% of the heating demand, considering the use of waste and residue biomass. This contribution is accounted for by subtracting the corresponding consumption (approximately 20 TWh_{LHV}/y) from the quantity of domestic biomass available for power generation and biofuel production.

District heating is assumed to cover 15% of the thermal demand from heating in the residential and services sector, defining the potential according to the methodology presented in Ref. [101]. The approach considers district heating from geothermal energy, biomass, thermoelectric power generation, and industry. District heating that utilises shallow geothermal sources is assisted by heat pumps, whose electricity consumption is included in the exogenous demand term. The district heating demand covered by thermoelectric power plants imposes a corresponding electricity generation term, which is endogenously computed in the model selecting either CCGTs or OCGTs, depending on the region and on the energy vector balances. This also sets a lower boundary for the installed capacity of such technologies.

Cooling introduces an electricity demand term, which is exogenously computed as a regional hourly-resolved profile, accounting for the needs related to indoor thermal comfort. The estimation takes into account a climatic variable known as Discomfort Index (function of environmental conditions like humidity, temperature, and solar irradiance), the time step (day of the week and month), and the location. Data have been obtained on a 11x11 km grid and then aggregated at regional scale. This is then translated into an electric consumption according to the expected long-term performance parameters of air conditioning units. The assessment results in an electricity demand of 32 TWh_e/y. Further investigation is left to future work.

3.1.2. *Transport*

The analysis considers the energy vector demand from the entire transport sector, including light mobility, heavy-duty transport, navigation, and aviation. For each segment, demand shares are defined according to recent prediction for the long-term evolution of the sector [2,103].

Table 4 shows the assumptions for road transport. Light mobility largely relies on BEVs, whose stock share is 75% for passenger cars and 50% for light-duty vehicles, compared to 15% and 25% for FCEVs and 7% and 15% for liquid fuel-based internal combustion engine vehicles (ICEVs). Due to different energy densities, energy vector demand shares are more balanced than stock shares, as noticeable by comparing the light mobility column in Fig. 4 (which includes passenger cars and light-duty vehicles) with Table 4. FCEVs and ICEVs are prevalent in heavy-

Table 4
Road transport stock share, consumption, stock, and mileage in the investigated long-term scenario, based on Refs. [24,106–112].

Category	ICEV-LF	ICEV-CH_4	BEV	FCEV	Stock	Mileage [km/y]
Passenger cars	10% 4 L/100 km	– –	75% 12.5 kWh_e/100 km	15% 0.6 kg_{H2}/100 km	24 millions	13,500
Light-duty vehicles	20% 11 L/100 km	5% 7 kg_{CH4}/100 km	50% 25 kWh_e/100 km	25% 3 kg_{H2}/100 km	4 millions	25,000
Heavy-duty vehicles	20% 29.2 L/100 km	10% 25 kg_{CH4}/100 km	10% 120 kWh_e/100 km	60% 7.5 kg_{H2}/100 km	700,000	100,000
Buses	15% 32 L/100 km	– –	50% 140 kWh_e/100 km	35% 8 kg_{H2}/100 km	113,000	45,000

duty transport, where they account for 60% and 20% of the stock, respectively. The current reliance of part of road transport on pure CH_4 is kept, with use of either natural gas or biomethane. The electricity consumption of BEV charging is assigned with hourly resolution [104], repeating a day-long profile shape that is assumed the same in each region, while a flat demand is assumed for the other energy vectors, as they can rely on well-established storage systems both at production sites and refuelling stations. A progressive improvement of average fuel efficiencies is assumed, considering the technology evolution towards high-performance solutions in the long term.

In road transport, the demand of energy vectors is computed taking into account average fuel efficiencies, average mileages, and the vehicle stocks. In accordance with long-term strategies [105], the analysis assumes that the stock of passenger cars will decrease by 40% while that of buses will increase by 10%, accounting for a modal switch towards public transportation and car sharing solutions. Correspondingly, the mileage of passenger cars and buses are assumed to increase by 20% and 10%, respectively. For heavy-duty transport, a reduction of milage is assumed from improved logistic management, as envisaged by national strategies [105]. The national demand is then disaggregated to the regions to comply with the spatial resolution of the model (see Section 3.4). The same distribution of the existing stock is considered for buses and heavy-duty transport, while light mobility demand is allocated according to population, population density, car stock, and average income per capita [24].

As Fig. 4 shows, electrification is modest in aviation and navigation, which mostly rely on liquid fuels, envisaging the replacement of oil derivatives with synthetic fuels [5,6,113]. Demand shares are assigned considering the national consumption for both national and international aviation and internal and maritime navigation, taking into account passenger and freight transport [114]. The resulting national energy vector demand is distributed geographically according to traffic data of airports and ports [115,116].

3.1.3. Industry

The projected industrial demand of energy vectors is built from historical consumptions, considering the sector evolution towards clean technologies. In particular, the analysis separately addresses the energy vector demand for process heat generation and feedstock, while making distinct assumptions for primary steelmaking and cement production. The resulting variation of the demand of energy vectors with respect to today's status is summarised in Fig. 5. Data on current consumptions in industrial sectors are retrieved from the JRC-IDEES database of the European Commission [117].

The analysis assumes direct electrification with industrial heat pumps of low-temperature process heat (<100 °C) for all sectors [8], excluding biomass-, geothermal-, and solar-based heat generation, which are kept equal to current values. As a result, the electricity demand features an additional contribution of 2.8 TWh_e/y, while the natural gas and oil derivatives demand are decreased by 7.5 TWh_{LHV}/y and 1 TWh_{LHV}/y, respectively. Medium- and high-temperature (greater than 100 °C) process heat generation based on natural gas, solid fuels, and oil derivatives is assumed to be converted to gas systems fed by a CH_4-H_2 blend. The resulting CH_4-H_2 demand is 103 TWh_{LHV}/y, while the natural gas, oil derivatives, and solid fuels consumptions decrease by 81 TWh_{LHV}/y, 16 TWh_{LHV}/y, and 2 TWh_{LHV}/y, respectively.

The evolution of the chemical industry involves the switch from conventional fossil-based feedstock to carbon–neutral solutions. The main chemical products are chlorine, ammonia, methanol, high-value chemicals (HVC, which include ethylene and propylene), and BTX (which include benzene, toluene, and xylenes) [9]. Chlorine production is already based on electricity, thus not requiring the introduction of specific assumptions. Natural gas is the most relevant feedstock of ammonia production. Since the synthesis process involves the reaction of hydrogen and nitrogen, the alternative low-carbon feedstock consists of pure hydrogen. Accordingly, ammonia production is assumed to switch from natural gas to hydrogen, considering a hydrogen requirement of 178 kg_{H2}/t_{NH3} [9]. Methanol is also produced from natural gas, which is reformed to H_2 that then reacts with CO_2 or CO. Consequently, the alternative low-carbon pathway is the hydrogenation of CO_2 with pure H_2, which requires 189 kg_{H2}/t_{MeOH} and 1.373 t_{CO2}/t_{MeOH} [9]. The production of both HVC and BTX is based on cracking of naphtha and, in a smaller fraction, of liquefied petroleum gas (LPG). The most relevant alternative low-carbon pathway is based methanol conversion to olefin or aromatics. Accordingly, the analysis assumes the conversion of the consumption of naphtha and LPG to methanol, which covers both HVC and BTX production and results in an additional demand of liquid fuels in the model. To estimate such demand, the methanol requirement for ethylene production is considered as reference (2.83 t_{MeOH}/t_{HVC} [9]), in accordance with the approach adopted in the European JRC-IDEES database [117]. The evolution of the Italian chemical industry results in additional demands of hydrogen, liquid fuels, and CO_2 of 7 TWh_{LHV}/y, 38 TWh_{LHV}/y, and 800 kt_{CO2}/y, while the corresponding decrease of natural gas, naphtha, and LPG consumptions are 7 TWh_{LHV}/y, 28 TWh_{LHV}/y, and 6 TWh_{LHV}/y.

Primary steelmaking is currently based on blast furnaces fed with

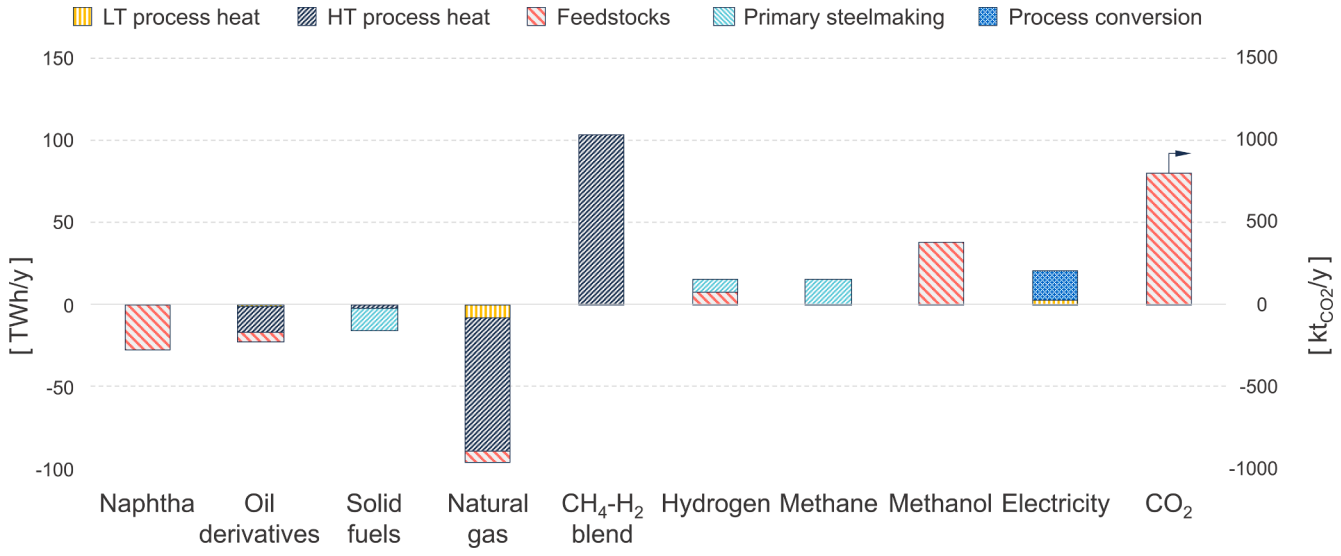

Fig. 5. Evolution of the industrial sector towards decarbonised technologies: impact on the demand of energy vectors.

coal, which serves as both heat source and carbonaceous feedstock. The existing facilities are assumed to switch to Direct Reduction of Iron ore (DRI) and Electric Arc Furnaces (EAF), considering that, as DRI feed, half of the production relies on methane and half on hydrogen. For the methane-based production, the implementation of CO_2 capture and storage is imposed. Overall, the decarbonisation of primary steelmaking feeds yields additional demands of hydrogen and methane of 7 TWh_{LHV}/y and 15 TWh_{LHV}/y, respectively, while avoiding the consumption of 14 TWh_{LHV}/y of coal (additional information regarding technical process data is available in Supplementary Material).

Cement production is one of the highest-emitting industrial processes, featuring significant process-related CO_2 emissions associated to the calcination reaction [118]. This work assumes the implementation of CO_2 capture and permanent sequestration to abate such emissions, as it is typically indicated as the main decarbonisation path for the sector [119,120]. As a result, 15 Mt_{CO2}/y are captured and permanently stored (additional information regarding technical process data is available in Supplementary Material).

The modification of production processes (chemicals, steel, and cement) yields an additional electricity demand of 17 TWh_e/y, excluding the contribution of the electrolysis consumption. For each subsector, the resulting demand of energy vectors is regionalised based on the regional distribution of value added [121]. A few exceptions are discussed in Supplementary Material. Finally, note that, as presented in Section 2.3.5, the production of biofuels and e-fuels for transportation is endogenously modelled; hence, the related consumptions of biomass, hydrogen, and CO_2 are not assigned as exogenous demand.

3.2. Power generation

The analysis considers the evolution of the power generation sector towards a massive penetration of renewable energy sources, introducing upper boundaries on the installed capacity of the included technologies. Solar photovoltaic (PV) and wind onshore are expected to feature the largest deployment. The potential of the former is set at 405 GW_e, and is estimated considering the possibility of rooftop- and ground-based plants, as well as installations on parking, quarries, landfills, motorways, and railways. The available wind speed and the geomorphological features of the territory set the onshore wind potential at 224 GW_e.

Offshore wind development is highly uncertain, since past studies strongly limit the potential due to deep waters. However, interest on the technology has risen in recent years due to the impellent need for renewables and the expected advancements in floating wind turbines, whose implementation might vastly enlarge the potential. Here, the analysis assumes an offshore wind power generation capacity of 9.5 GW_e, which was determined considering areas with suitable wind intensity and seabed morphology for piled foundations [24]. Further assessments will investigate additional suitable areas and related installation potential. In accordance with the national strategies, which consider that most available areas have already been exploited, a slight increase is assumed for geothermal and hydroelectric power generation capacities, reaching 1 GW_e for geothermal, 25 GW_e for reservoir and run-of-river hydropower, and 7 GW_e and 700 GWh_e for pumped hydro [105,122]. The analysis assumes to saturate the potential capacities of offshore wind, geothermal, and hydro technologies. This does not significantly impact the system configuration since most of the capacity derives from the revamping of existing plants and additions are modest compared to those observed for PV and onshore wind.

For thermoelectric power generation, the analysis assumes the phase out of oil-based and coal-based plants. The revamping of CCGTs and OCGTs is considered, with the installation of high-efficiency devices fuelled by CH_4-H_2 blend. The maximum capacity is set 50% higher than current values, as revamping generally involves larger machinery (resulting in 83 GW_e for CCGT and 5 GW_e for OCGT). The upper boundary for biomass-based power generation is assumed equal to today's status (4 GW_e), since its evolution competes with the food sector and with biofuel production. At any rate, the main constraint is the limited availability of biomass (see Section 3.3). Waste-to-Energy (WtE) plants are assumed to be kept, with unvaried installed capacity (1 GW_e) and fixed feedstock quantities, according to national strategies that maintain incineration as a main option to manage residual waste [123].

3.3. Domestic sources and imports

The availability of domestic sources strongly affects the energy system configuration, as different sectors are in competition for the consumption of limited amounts. This work sets as upper boundary for the domestic natural gas production the 2019 value (47 TWh_{LHV}/y), considering both onshore and offshore wells [124]. The biomass availability is determined considering exclusively waste and residual solid biomass (52 TWh_{LHV}/y, net of the quantity dedicated to heating), thus avoiding competition with the food sector and complying with the principles of sustainable production and environmental protection [125]. All biogas produced from livestock residues and biodegradable fraction of municipal waste is assumed to be upgraded to biomethane (55 TWh_{LHV}/y [125,126]), and the CO_2 that results from the upgrading process (8 Mt_{CO2}/y) is assumed available for sequestration or usage. Permanent sequestration of CO_2 is also constrained by an upper boundary, as Italy is endowed with a limited availability of potential storage sites. Specifically, the analysis assumes a maximum annual storage capacity of 20 Mt_{CO2}/y, which corresponds to the lower boundary of the range indicated in the national long-term strategy (LTS) [105].

To account for energy security and independence issues, a set of strategic constraints involving boundaries on imports is introduced in the analysis. Specifically, the domestic production of hydrogen is imposed to represent at least 70% of the total consumption, while blue hydrogen is constrained to supply 10% of consumption to ensure diversification of sources. Similarly, the domestic production of sustainable liquid fuels (i.e., biofuels and e-fuels) is imposed to cover at least 10% of consumption. The strategic position of Italy within Europe is considered by introducing the transfer of hydrogen towards northern EU countries (1.5 Mt_{H2}/y, corresponding to 50 TWh_{LHV}/y), thus accounting for the development of the supply corridor with North Africa envisaged in the strategies of the European Union [127–129].

3.4. Network topologies

The case study implementation considers a regional subdivision of the Italian territory, with nodes corresponding to NUTS-2 level elements. As a results, each energy vector network is composed of 20 nodes, which are represented in Fig. 6. All the model input data, such as the demand of energy vectors, the RES potential, and the domestic sources availability, are regionalised according to the adopted spatial resolution, as detailed in Supplementary Material.

Fig. 7 summarises the topology of the energy vector transport networks. The electricity network (Fig. 7.a) is built considering the structure of the existing grid and planned additional connections. Power transfer limits across country borders and between regions are introduced based on the long-term projections of the TSO [96]. Given that the Italian electricity TSO provides transport limits between bidding zones, the model implementation considers the aggregate of the exchanges between the regions that belong to different zones (see Supplementary Material for additional information). Based on the adopted approach, grid expansion is not endogenously optimised, as the related transport capacity limits are assigned exogenously, considering the envisaged upgrades. In this way, model results enable an assessment of the effectiveness of such interventions, identifying which connections are stressed the most. The endogenous optimisation of grid capacity expansion is foreseen in future development of the work.

The existing and planned connections of today's natural gas grid are considered to define the gas network topology [130]. Employing the

Fig. 6. Geographical subdivision of the Italian territory according to NUTS-2 regions, as implemented in the model. Region abbreviations are reported in the Nomenclature.

same approach implemented for the electric grid, volumetric transport capacity limits are exogenously introduced based on the size of existing and planned natural gas pipelines [131], assuming that they will be repurposed to deliver a CH_4-H_2 blend with unconstrained hydrogen fraction [96]. In other words, the retrofitting of the existing gas grid enables gas transport with no limits on the hydrogen fraction, in line with the roadmap of the transmission system operator [132]. This implies that the infrastructure can be exploited to deliver pure hydrogen as well, the only constraint being the available transport capacity.

The transport network of pure hydrogen represents the development of a dedicated delivery infrastructure, which may be required in the case the transport capacity of the gas network is saturated. Accounting for the development of a new infrastructure, connections between all adjacent regions are enabled. These consider a non-detailed combination of pipeline, truck, and ship delivery using an average transport cost, since the optimal selection of the transport technology depends on multiple factors (e.g., morphological features of the territory, spatial distribution of demand points), as previously investigated by the authors [133,134]. The scenario assumes the possibility of underground hydrogen storage in all nodes, except for mountain regions (LIGU, TREN, VALL, referring to Fig. 6), for which this option appears impractical. Since the analysed case study is mainly intended to demonstrate the model capabilities and potential, the detailed assessment of underground storage potential is deferred to future assessments aimed at providing system development recommendations. Accordingly, a specific investment cost of 25 €/kg_{H2} is considered, representative of the average between lined rock cavern solutions, which offer higher flexibility in terms of suitable locations and structural requirements, and storage in geological formations such as depleted gas fields or salt caverns [135].

Import points for natural gas and hydrogen are selected based on existing infrastructures. In particular, cross-border pipeline connections are exploited to import a blend of natural gas and hydrogen, which share the existing import capacities [136], as indicated in Fig. 7.b. The existing and planned regasification facilities are considered for the import of liquefied natural gas (LNG) [137], and the same locations are selected as candidate import points for liquid hydrogen (LH_2), assuming an average capacity of 25 MSm^3/d. Regarding the origin of the energy vector, green H_2 from North Africa is delivered exploiting the pipeline connections in Sicily (SICI in Fig. 6) to account for the development of the corridor with Europe [127], whereas all the other pipeline entry points can be exploited to import blue H_2. Liquid H_2 import points feature both green and blue hydrogen, as this option offers higher flexibility in terms of point of origin.

Liquid fuel transport relies on a well-established infrastructure, with connections between all adjacent regions. Coastal regions featuring the main freight ports are selected as entry points for imports. Regarding the energy vector origin, both oil-based and carbon–neutral fuels can be imported in any of the selected regions, without any constraint on quantities.

Table 5 summarises the main assumptions related to energy vector imports and transport within the domestic networks. As discussed in Section 2, OMNI-ES encompasses both the energy vector import costs and the CO_2 emissions of the related supply chains, thus avoiding possible carbon leakages from out-of-model-boundary processes. On the other hand, as described in Section 2.3.1, transport costs encompass the annual aggregate expenses sustained by transmission system operators, comprising operational expenditures and investments for infrastructure developments.

4. Results and discussion

The OMNI-ES model is applied to investigate the presented long-term scenario for Italy, which considers 2050 as target year and requires the achievement of carbon neutrality. Provided the network topologies, the exogenous demand of energy vectors, and the upper boundaries on the availability of sources, the model optimises the multi-sector energy system in terms of installed capacities (of both conversion and storage systems) and hourly flows of energy vectors and CO_2.

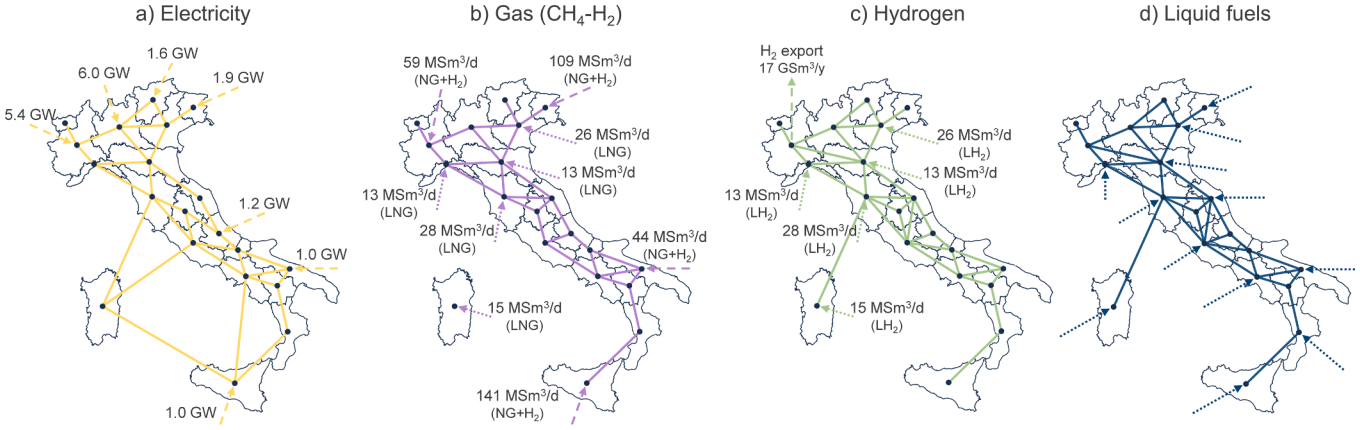

Fig. 7. Transport network topologies. Arrows indicate entry/exit points for import/export.

Table 5
Input data regarding import and transport of energy vectors.

		Value	Unit	Ref.
Electricity import	Cost	100	€/MWh_e	Assumed
	Supply chain emissions	100	g_{CO2}/kWh_e	[138]
Natural gas import	Cost	50	€/MWh_{LHV}	Assumed
	Supply chain emissions	54	g_{CO2}/kWh_{LHV}	[139]
Green hydrogen import	Cost	2	€/kg_{H2}	[140]
	Supply chain emissions	0	kg_{CO2}/kg_{H2}	–
Blue hydrogen import	Cost	3	€/kg_{H2}	[141]
	Supply chain emissions	3	kg_{CO2}/kg_{H2}	[138]
Carbon-neutral liquid fuel import	Cost	1.4	€/L	[142]
	Supply chain emissions	0	g_{CO2}/kWh_{LHV}	–
Oil-derived liquid fuel import	Cost	0.7	€/L	[143]
	Supply chain emissions	72	g_{CO2}/kWh_{LHV}	[139]
Electricity transport	Cost	27.6	€/MWh_e	[144]
Gas (CH_4-H_2 blend) transport	Cost	2.7	€/MWh_{LHV}	[144]
Hydrogen transport	Cost	15	€/MWh_{LHV}	[133,145]
Liquid fuel transport	Cost	2.2	€/MWh_{LHV}	[146]

This section presents and discusses the results obtained for the case study presented in Section 3, while Section 5 investigates sensitivity analyses on the availability of CO_2 storage capacity and on the upper boundary of liquid fuel import. The computational time required to solve the LP problem ranges between 5 and 24 h depending on the analysed scenario, using a machine equipped with Intel Core i9-10980XE processor and 64 GB RAM and the solver Gurobi™. The main features of the resulting cost-optimal national energy system are provided in Table 6 and analysed in detail in the remainder of this section.

4.1. Use of energy vectors in the integrated energy system

The total annual consumption of electricity results more than

Table 6
Main features of the resulting cost-optimal energy system configuration.

	Parameter	Value	Upper boundary
Energy vector total consumption	Electricity	787 TWh_e/y	–
	Hydrogen	305 TWh_{LHV}/y	–
	Methane	110 TWh_{LHV}/y	–
	Liquid fuels	153 TWh_{LHV}/y	–
Power generation capacity	Photovoltaic	313 GW_e	405 GW_e
	Onshore wind	130 GW_e	224 GW_e
	Offshore wind	9.5 GW_e	Assigned
	Geothermal	1 GW_e	Assigned
	Hydroelectric	25 GW_e	Assigned
	Biomass	2.4 GW_e	4.1 GW_e
	Waste-to-Energy	1 GW_e	Assigned
	Fuel cell systems	0 GW_e	–
	CCGT	13 GW_e	83 GW_e
	OCGT	5 GW_e	5 GW_e
H_2 production capacity	Electrolysis	192 GW_{LHV}	–
	SMR with CO_2 capture	0 GW_{LHV}	–
Storage capacity	BESS	111 GWh_e	–
	Hydrogen - Underground	883 GWh_{LHV}	–
	Hydrogen - Aboveground	190 GWh_{LHV}	–
	PHS	779 GWh_e	Assigned
	Liquid fuel storage	286 GWh_{LHV}	–
Domestic production	Natural gas	47 TWh_{LHV}/y	47 TWh_{LHV}/y
	Biomethane	55 TWh_{LHV}/y	55 TWh_{LHV}/y
	Biomass	52 TWh_{LHV}/y	52 TWh_{LHV}/y
Import	Natural gas	9 TWh_{LHV}/y	–
	Liquefied natural gas	0 TWh_{LHV}/y	–
	Green H_2 – Gaseous*	137 TWh_{LHV}/y	150 TWh_{LHV}/y
	Green H_2 - Liquid	0 TWh_{LHV}/y	
	Blue H_2	10 TWh_{LHV}/y	
	Electricity	55 TWh_e/y	–
	Oil-based LF	0 TWh_{LHV}/y	–
	Carbon-neutral LF	137 TWh_{LHV}/y	–
CO_2 technologies	Capture from power generation	0 Mt_{CO2}/y	–
	Capture from SMR	0 Mt_{CO2}/y	–
	Capture from biogas upgrading	4 Mt_{CO2}/y	8 Mt_{CO2}/y
	Capture from primary steelmaking	3 Mt_{CO2}/y	Assigned
	Capture from cement production	15 Mt_{CO2}/y	Assigned
	Direct air capture	0 Mt_{CO2}/y	–
	Usage in P2L	1.7 Mt_{CO2}/y	–
	Permanent storage	20 Mt_{CO2}/y	20 Mt_{CO2}/y
	Extra term (balance closure)	0 Mt_{CO2}/y	–

* Includes 50 TWh_{LHV}/y exported towards northern EU countries.

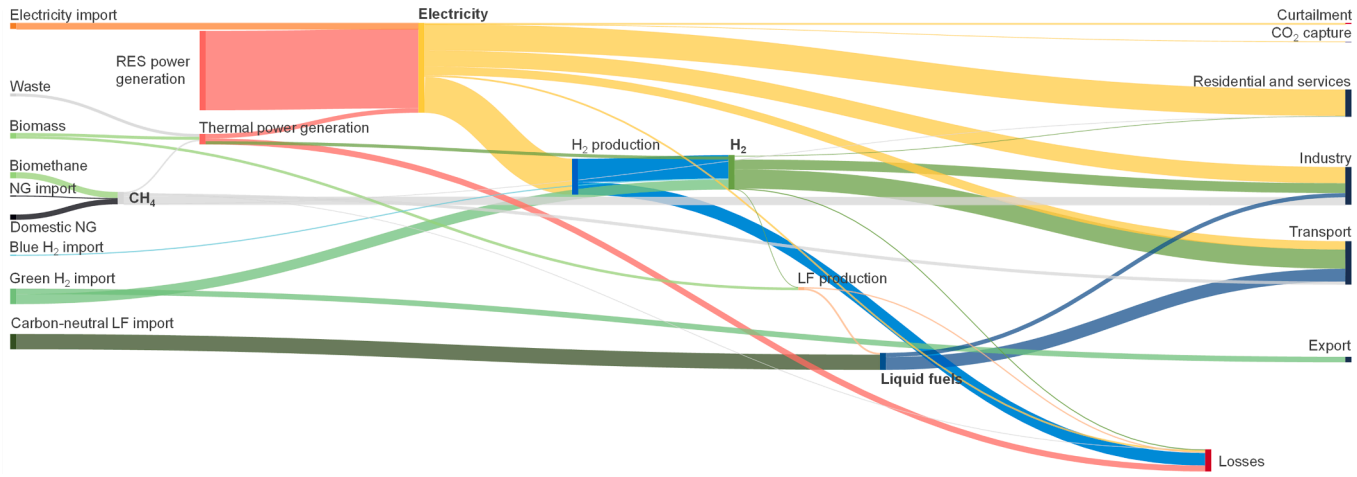

Fig. 8. Sankey diagram of the cost-optimal energy system configuration for the Italian case study. The role of hydrogen in energy storage can be noted via the "backward" flow to power generation.

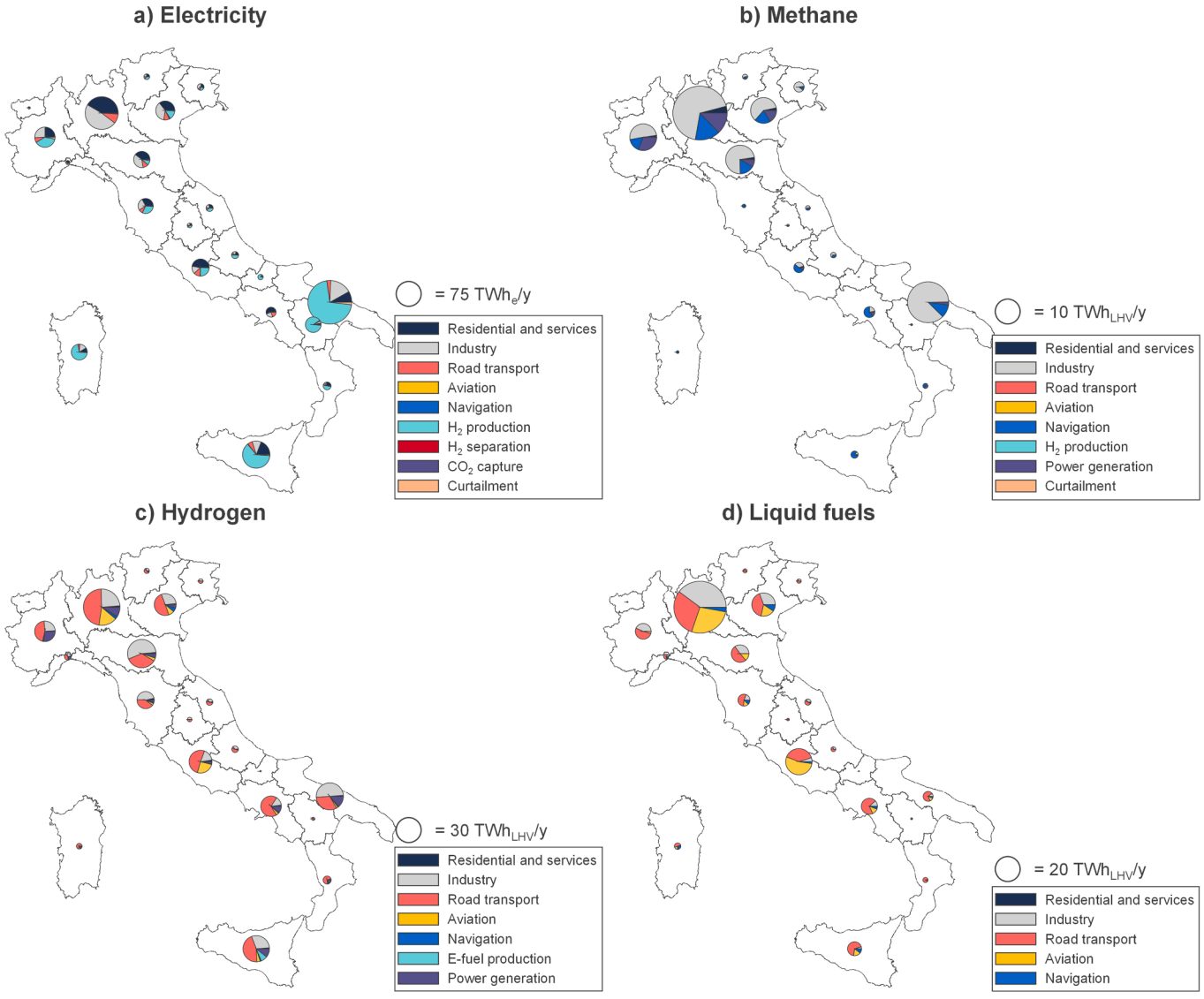

Fig. 9. Total annual energy vector consumption by region. Scales are different for each energy vector.

doubled compared to current values, reaching nearly 800 TWh_e/y. As the Sankey diagram in Fig. 8 shows, endogenous terms significantly contribute to the electricity consumption, which results nearly twice the exogenous demand (453 TWh_e/y). Excluding electrolysis consumption, the hourly peak load in the year is equal to 87 GW_e, whereas current values are in the order of 60 GW_e [147]. Despite the massive RES penetration, curtailment is limited to 10 TWh_e/y (approximately 1% of the total electricity generation), thanks to the availability of multiple storage technologies.

The production of green hydrogen strongly impacts the power sector, as electrolysis consumption accounts for 324 TWh_e/y. However, as Fig. 8 shows, energy vector flows are deeply interwoven. In such a highly integrated system, their contribution is about more than covering exogenous demands, as all the interactions serve for the system optimisation and complete decarbonisation, reflecting also the needs for storage and flexibility. Indeed, while the total hydrogen consumption is 305 TWh_{LHV}/y (9 Mt_{H2}/y), approximately 30 TWh_{LHV}/y are converted back to electricity and 3 TWh_{LHV}/y to e-fuels. As a result of the limited availability of biomethane (approximately 55 TWh_{LHV}/y), the average hydrogen fraction in gas (CH_4-H_2 blend) amounts to 60% at end uses in the residential and services and industrial sector, 70% at CCGTs, and 85% at OCGTs (on energy basis).

The domestic availability of biomethane is entirely exploited, resulting in 50% of the total annual consumption of methane (55 TWh_{LHV}/y of biomethane over a total of 110 TWh_{LHV}/y). The CH_4 fraction in blend uses is limited, amounting to 55 TWh_{LHV}/y in end-use sectors (residential and services and industry) and 13 TWh_{LHV}/y in thermoelectric power generation. The remainder is used in processes that require pure CH_4, such as primary steelmaking (15 TWh_{LHV}/y) and road mobility (28 TWh_{LHV}/y). Domestic production of blue hydrogen is absent, as the system favours biomethane uses in other applications and CO_2 capture on other processes. The use of biomethane in systems with carbon capture enables the availability of biogenic CO_2 that can be either converted to carbon–neutral fuels or sequestered to implement carbon sinks.

The consumption of liquid fuels is entirely covered by carbon–neutral options, either domestic or imported. In the resulting cost-optimal energy system, biofuel production accounts for approximately 13 TWh_{LHV}/y, consuming nearly 24 TWh_{LHV}/y of solid biomass, while the total e-fuel production corresponds to 3 TWh_{LHV}/y, consuming approximately 3 TWh_{LHV}/y of H_2 and 0.9 Mt_{CO2}/y of CO_2. The exogenous demand of green industrial feedstocks introduces an additional requirement of 0.8 Mt_{CO2}/y of CO_2. Overall, neutral CO_2 is entirely from biogenic origin, since DAC is not exploited in the cost-optimal energy system. Similarly to today's status, the system heavily relies on import, saturating the upper boundary (90% of the final demand, corresponding to 136 TWh_{LHV}/y). A higher degree of energy independence would require further installations of RES power generation to support the additional green hydrogen production and DAC consumption. Indeed, the available solid biomass potential would only be sufficient to obtain 28 TWh_{LHV}/y of biofuels, thus requiring an increased production of e-fuels. The latter should mostly employ CO_2 obtained via DAC, since the amount of CO_2 that can be retrieved from biogenic sources (excluding solid biomass that is assumed exploited for biofuel production) would limit the e-fuel production potential to approximately 60 TWh_{LHV}/y.

Fig. 9 shows the regional distribution of energy vector consumptions, highlighting the contributions of the different sectors. All energy vectors feature significantly higher consumptions in northern regions for all sectors. Exceptions are the electrolysis consumption, which is concentrated in southern regions in correspondence with the larger RES availability, and primary steelmaking, whose consumption of methane and hydrogen is entirely located in the Apulia region (PUGL in Fig. 6).

The hydrogen consumption encompasses uses from both the gas grid, in which it is blended with methane, and the hydrogen infrastructure, in which it is delivered as pure. As observed also in Fig. 8, the hydrogen consumption is significantly higher than methane (note that scales in Fig. 9 are different for each energy vector), due to the constrained availability of biomethane and the limited CO_2 storage capacity.

Liquid fuel consumption is primarily driven by demand of heavy-duty transport, aviation, and industrial feedstocks. As such, uses are concentrated in regions in the northern part of the country, which are characterised by a considerably larger presence of industrial activity, and in those that feature the main airports.

4.2. Power generation

To comply with the increase in electricity consumption and the low capacity factor of the most abundant RES-based technologies, the full decarbonisation of the multi-sector national system requires a RES power generation capacity in the order of hundreds of GW. PV and onshore wind are the only options that feature such a large potential in Italy, whereas the margin of exploitation of other renewables (offshore wind, geothermal, and hydroelectric, including PHS) is limited to dozens of GW. Accordingly, the capacity of hydroelectric, offshore wind, and geothermal power generation is assigned to the upper boundaries discussed in Section 3.2, as their impact on the overall system configuration is modest. In addition, the considered values (reported in Table 6) are in accordance with official Italian long-term projections such as National Energy and Climate Plan (NECP) [122] and LTS [105]. The biomass power generation capacity is included as decision variable considering the possible revamping of existing plants, in order not to implicitly favour it over biofuel production.

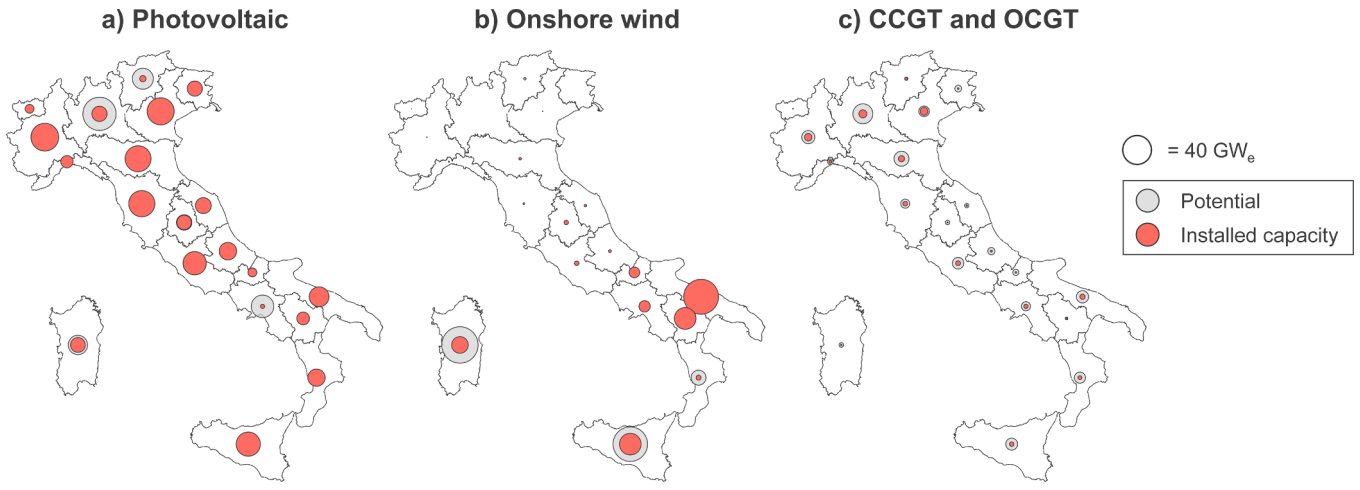

Fig. 10. Installed capacity and available potential of photovoltaic (a), onshore wind (b), and gas turbine-based (c) power generation.

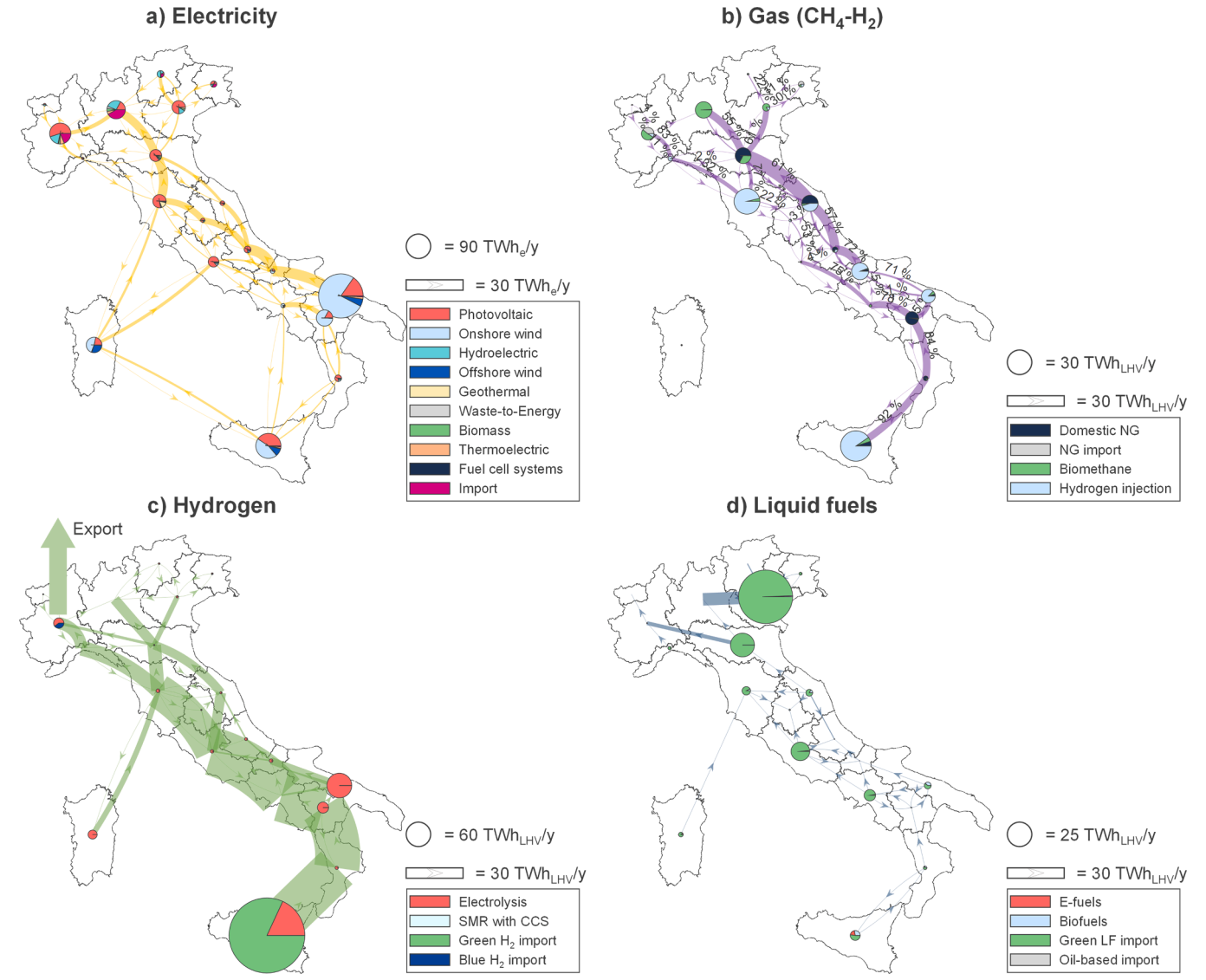

Fig. 11. Total annual energy vector generation and transport. Pies indicate the annual generation by region, and the scale is different for each network. The width of connection edges represents the total annual quantity transported between regions. Percentages in the gas network represent the annual average hydrogen fraction in the blend for each connection (on energy basis).

The resulting system features massive installations of PV and onshore wind, which are close to saturation in most regions, as shown in Fig. 10. Photovoltaic power generation (Fig. 10.a) is distribute rather homogeneously, and its potential is almost completely exploited except in regions characterised by less favourable solar irradiance. On the contrary, the onshore wind (Fig. 10.b) potential is almost entirely located in the southern part of the country, where it is exploited to a lesser extent in regions that feature a combination of relatively lower capacity factor and electricity consumption.

Thermoelectric power generation via CCGTs and OCGTs (Fig. 10.c) features a combined installed capacity of 18 GW$_e$, mainly located in northern regions, which are characterised by higher electricity demand and lower RES availability. In the resulting energy system, these plants mainly operate to cover RES generation deficits and to meet the district heating thermal demand. In such conditions, the system saturates the upper boundary of OCGTs capacity (5 GW$_e$), as the lower investment cost for revamping compensate the worse efficiency. As expected, fuel cell systems are not exploited, since both CCGTs and OCGTs can be fed by gas with unconstrained hydrogen fraction and fuel cells feature higher investment costs (than both CCGTs and OCGTs) and lower efficiency (than CCGTs). However, this option may become relevant in medium-term scenarios (e.g., considering the year 2030) with limited hydrogen fraction in gas turbine combustors, in possible local uses, or in providing grid services [148].

4.3. Energy vector transport and infrastructure requirements

Fig. 11 shows the generation and transport of energy vectors in their respective networks. Electricity (Fig. 11.a) generation in southern regions is mostly based on onshore wind, where it features both larger installed capacity and higher capacity factors than photovoltaic. Overall, such regions mostly rely on renewable power generation, benefitting from a richer sources endowment (solar radiation, onshore, and offshore wind). Photovoltaic generation is predominant in the northern part of the country, which features lower capacity factors compared to southern regions but large potential for installations thanks to the wide availability of free surfaces. Hydroelectricity also provides a significant contribution, whereas wind power generation is nearly absent in this area. The two import points in Piedmont and Lombardy (PIEM and LOMB in Fig. 6, respectively) are widely exploited, while gas turbine- and biomass-based power generation provide comparable but relatively minor contributions if compared to other technologies, being hardly

Table 7
Energy capacity and equivalent operating cycles of storage systems.

Technology	Energy capacity	Equivalent operating cycles [-]
BESS	111 GWh_e	316
Hydrogen – Underground	883 $GWh_{LHV,H2}$	16
Hydrogen – Aboveground	190 $GWh_{LHV,H2}$	221
PHS	779 GWh_e	17
Liquid fuels storage	286 $GWh_{LHV,LF}$	33

visible in Fig. 11.a. Despite the uneven source distribution, power generation is fairly balanced in the country. As a result, the need to transport electricity over long distances is moderate if compared to the other energy vectors.

The gas network, which, as discussed in 2.3.3, is representative of the existing gas grid, features high hydrogen fractions, with some connections exceeding 90% as annual average (Fig. 11.b). The main hydrogen injection points are located in regions with large H_2 production or import and that feature connections with sufficiently large capacity. Tuscany (TOSC in Fig. 6) collects green hydrogen produced in Sardinia (SARD in Fig. 6), which is not connected to the mainland with gas pipelines, to deliver it to northern regions. As Table 6 shows, the domestic availability of both natural gas and biomethane is fully exploited (dark blue and green in Fig. 11.b, respectively), whereas natural gas import is marginal if compared to today's status (9 TWh_{LHV}/y compared to over 700 TWh_{LHV}/y, corresponding to approximately 750 MSm^3/y and 70 GSm^3/y [149]). In addition, liquefied natural gas import is not exploited due to the higher cost and the limited use of fossil methane.

The system tends to saturate the available transport capacity of the gas grid, as it offers a lower transport cost, avoiding the need for capital expenses. Indeed, many connections are operated at the full pipeline capacities for nearly 8000 h per year. Such behaviour is especially observed in northbound connections in southern regions, where hydrogen is largely available and demand is limited if compared to northern regions. Overall, the required hydrogen flows exceed the available transport capacity of the existing gas grid, requiring the use of new installations, which are represented by the pure hydrogen infrastructure (Fig. 11.c).

Hydrogen production and import are mostly located in the southern part of the country, thanks to the availability of renewable sources and to the connection with North Africa, which guarantees green H_2 at low cost. As a result, the system features south-north corridors to deliver hydrogen towards the main consumption points in northern regions. In addition, the hydrogen infrastructure ensures the transport of 50 TWh_{LHV}/y imported from North Africa through Sicily (SICI in Fig. 6) to northern European countries. According to the assumed techno-economic parameters, green hydrogen import is more cost-effective than domestic production, and the system saturates the imposed upper boundary (30% of consumption). The pipeline connection in Sicily (SICI in Fig. 6) is the only entry point, as liquid hydrogen import is not exploited due to the higher cost. The cost-optimal system does not include hydrogen separation from the gas blend, since the process is more expensive than transporting pure hydrogen and would introduce additional electricity consumption.

Import of carbon–neutral liquid fuels is favoured over domestic production (Fig. 11.d), which results more expensive according to the adopted techno-economic assumptions and sources availability. On the one hand, the limited biomass potential constrains the production of biofuels, which also competes with biomass-based power generation. On the other hand, e-fuel production introduces important requirements for additional hydrogen production and neutral CO_2, strongly impacting also the power sector. Thanks to the wide distribution of import points, the system features modest needs for liquid fuel transport among regions, favouring importing regions closer to the main demand hubs in the northern part of the country. However, liquid fuel transport may become relevant in scenario with higher energy independence, as source points would shift towards regions with larger availability of biomass and low cost H_2 and CO_2. Further details on the resulting energy vector transport networks are provided in Supplementary Material.

4.4. Storage requirements

As reported in Table 6, storage systems are widely exploited to support the massive penetration of renewables and the consequent mismatches between supply and demand. Table 7 contains a focus on the size and operation of storage units in terms of installed energy capacity and equivalent operating cycles. BESS are exploited to cover short-term oscillations of the electricity balance, as their installed capacity is smaller if compared to other options and they are frequently cycled. Indeed, such systems are completely emptied nearly on a daily basis, with 316 equivalent cycles per year.

The system makes significant use of underground hydrogen storage to compensate long-term mismatches. This option exceeds 800 $GWh_{LHV,H2}$ of capacity and features, on average, complete discharges approximately on a monthly basis (16 equivalent operating cycles per year). A similar behaviour is observed for PHS, which features a cumulative capacity of 779 GWh_e (assigned, as discussed in Section 4.2) and an average of 17 equivalent cycles per year (optimised by the model).

Aboveground hydrogen storage is exploited in regions with unavailability of underground options. The higher investment cost limits the installed capacity to 190 $GWh_{LHV,H2}$. The possibility to implement higher charge and discharge rates allows this option to be cycled more frequently, reaching 221 equivalent cycles per year.

As example of the operation of storage systems, Fig. 12 shows the hourly evolution of the storage content of one facility for each technology. Specifically, the figure shows the year-long profile of seasonal systems (underground hydrogen storage and PHS) and the weekly operation of short-term options, extracting two representative weeks, for summer (red) and winter (light blue), respectively. In particular, the third week of June and the third week of December are considered. It can be observed that the considered underground hydrogen storage site (Fig. 12.a) is cycled on a monthly basis, and it is characterised by a larger storage content on average during summer, when solar radiation is largely available. Seasonality is more pronounced in the analysed PHS system (Fig. 12.b), which is completely emptied in January and refilled from April to June, featuring 5 equivalent cycles per year[1]. The operation of aboveground hydrogen storage (Fig. 12.c) and BESS (Fig. 12.d) is driven by photovoltaic generation, as they are characterised by a strong daily pattern. Such behaviour is especially evident for batteries in the summer week, when they are fully charged and discharged on a daily basis. Conversely, winter week profiles are less regular, featuring entire days without charging, and hourly fluctuations during daytime.

Overall, the electricity output from BESS and PHS is equal to 32 TWh_e/y and 12 TWh_e/y, respectively. Such values are comparable with the electricity generation via hydrogen-fuelled gas turbine-based systems (17 TWh_e/y). Hydrogen reconversion to electricity thus has a valuable role in the studied long-term Italian integrated energy system, thanks to the possibility to store large quantities of energy for long periods without suffering from self-discharge losses.

Liquid fuels are stored in tanks, for a total capacity of 286 $GWh_{LHV,LF}$. For this energy vector, storage is exploited to compensate the oscillations of e-fuel production, which is constrained by the discontinuous availability of green hydrogen. While stricter energy independence requirements may increase the need for liquid fuel storage, this would have a minor impact on the energy system configuration and economic performance, given the low investment cost of such technology.

[1] For PHS, the analysis assumes a minimum storage content corresponding to 35% of the available capacity, in order to avoid complete emptying of basins. Accordingly, the profile shown in Fig. 12 refers to the available storage capacity, net of the constraint on the minimum storage content.

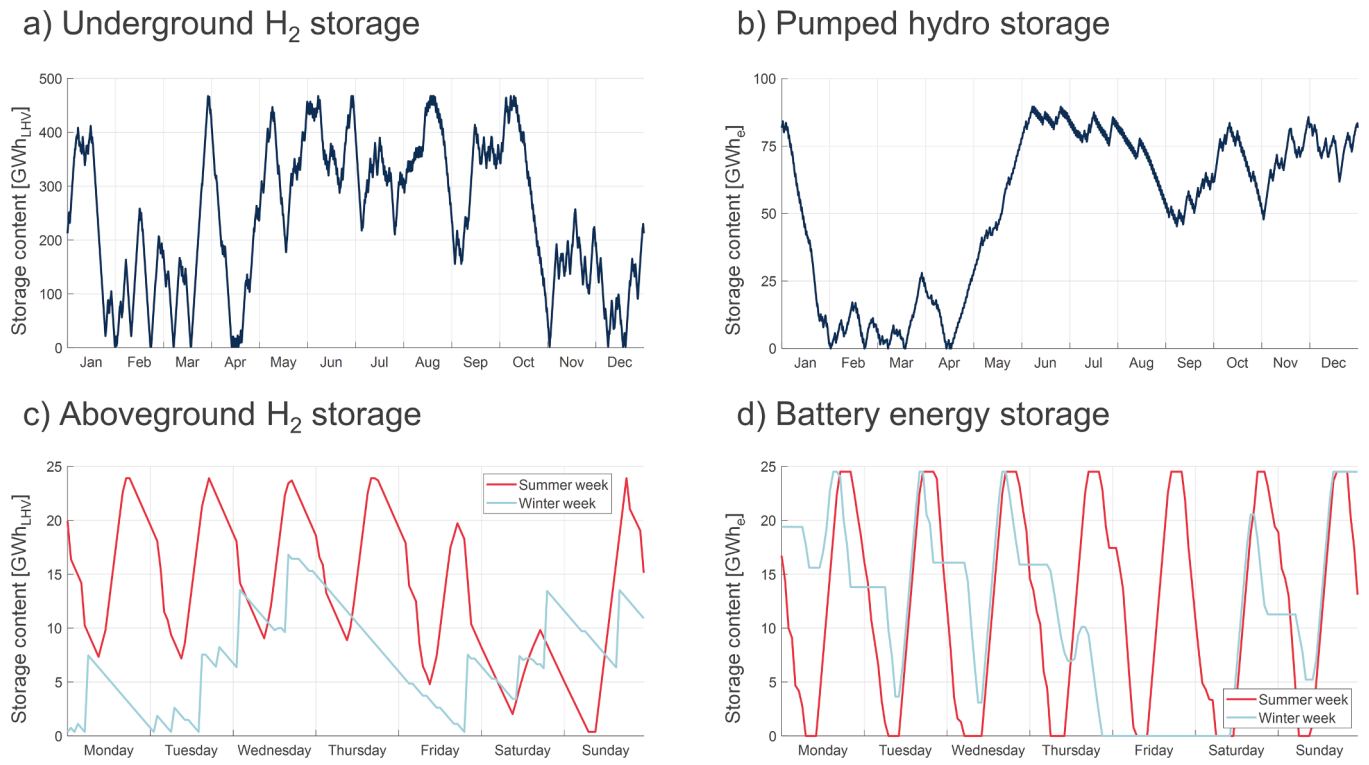

Fig. 12. Example of year-long or week-long hourly storage operation in selected facilities: a) underground hydrogen storage in PUGL; b) pumped hydro storage in ABRU; c) aboveground hydrogen storage in TREN; d) battery energy storage in TOSC.

Table 8
Annual CO_2 balance.

Category	Contribution	Value [Mt_{CO2}/y]
Fossil CO_2 sources	Natural gas	11.4
	Oil-based fuels	0
	Waste	4.7
	Supply chain-related emissions	10.7
	Unavoidable emissions*	38.2
	Total fossil CO_2 sources	**65.0**
CO_2 capture	CO_2 capture from biogas upgrading	3.7
	CO_2 capture from primary steelmaking	3.2
	CO_2 capture from cement production	14.8
	CO_2 capture from power generation	0
	CO_2 capture from SMR	0
	CO_2 capture from DAC	0
	Total CO_2 capture	**21.7**
CO_2 sinks	Permanent storage	20.0
	Natural absorption	45.0
	Total CO_2 sinks	**65.0**
CO_2 uses	E-fuel production	0.9
	Chemical industry feedstock	0.8
	Total CO_2 uses	**1.7**

* These include activities where CO_2 capture is not suitable and residual feedstock-related emissions resulting from incomplete capture in industrial processes where CO_2 capture is applied (e.g., 90–95% efficiency).

4.5. CO_2 balance

As Table 6 shows, the system achieves carbon neutrality by saturating the available CO_2 storage capacity, avoiding the use of the high-cost balance closure term. Table 8 details the annual CO_2 balance of the system, highlighting the contribution of the different sources, sinks, and uses. According to the carbon-neutrality constraint, all the fossil carbon that enters the system boundaries must be compensated. Sources of fossil origin (natural gas, oil-based fuels, waste) account for approximately 16 Mt_{CO2}/y, which may be captured according to the process in which they are employed. Supply-chain related emissions of the imported energy vectors exceed 10 Mt_{CO2}/y and are thus comparable with the amount of carbon directly introduced with the use of fossil fuels, stressing the importance of including this contribution. Unavoidable emissions amount to 38.1 Mt_{CO2}/y and include the contribution of agriculture, non-energy waste management, and process-related industrial emissions that do not derive from the energy vectors included in the model (as detailed in Supplementary Material), as well as the residual emissions of cement production and the non-energy emissions of primary steelmaking. Overall, the system needs to compensate 65 Mt_{CO2}/y of fossil CO_2, corresponding to approximately 15% of the total CO_2 emissions registered in Italy in 2019 (418 Mt_{CO2}/y [150]).

Compensation is attained through CCS and natural absorption. In particular, the former accounts for 20 Mt_{CO2}/y, corresponding to the saturation of the available annual storage capacity, while the latter amounts to 45 Mt_{CO2}/y. Natural absorption thus overcompensates unavoidable emissions, but the indirect emissions related to supply chains exceed the available negative carbon budget, balancing out the contributions. As a result, the system has no room for the use of fossil fuels with cost-free compensation.

Carbon capture is implemented on multiple technologies, covering both fossil and biogenic sources, for a total of 21.7 Mt_{CO2}/y. Of these, 20 Mt_{CO2}/y are sent to permanent sequestration, saturating the available annual storage capacity, while the remaining 1.7 Mt_{CO2}/y are used in e-fuel production (0.9 Mt_{CO2}/y) and as a feedstock for methanol production in the chemical industry (0.8 Mt_{CO2}/y). Regarding the CO_2 origin, 3.7 Mt_{CO2}/y are captured from biogas upgrading, 3.2 Mt_{CO2}/y from methane-fed primary steelmaking, and 14.8 Mt_{CO2}/y from cement production. Accordingly, the available storage capacity of 20 Mt_{CO2}/y is almost entirely saturated by the amount of CO_2 that must be captured from steelmaking and cement production, which cumulatively account for 18 Mt_{CO2}/y. The residual capacity is exploited for the sequestration of 2 Mt_{CO2}/y from biogas upgrading to obtain negative emissions, as it is economically favourable compared to the implementation of CO_2 capture on power generation systems. The remaining 1.7 Mt_{CO2}/y captured from biogas are used as carbon–neutral CO_2 feedstock in e-fuel and

Table 9
Sensitivity analyses on available CO_2 storage capacity and on the liquid fuel import limit: results variation compared to the baseline scenario.

	+100% CO_2 storage capacity	–33% liquid fuel import limit
PV capacity	−12%	+20%
Onshore wind capacity	−11%	+4%
NG consumption	+132%	−4%
H_2 consumption	−24%	+14%
E-fuel production	−85%	+1130%
Biofuel production	+13%	+116%
Total annual cost	−1%	+1%

methanol production. The system avoids the use of DAC, as the available biogenic CO_2 is sufficient to cover the required e-fuel production.

5. Sensitivity analyses

Results of the baseline scenario indicate that the system saturates the upper boundary of the available CO_2 storage capacity and of the import of carbon–neutral fuels. Such parameters warrant further investigation, as they are expected to be among the most impactful on the energy system optimal configuration. Indeed, a wider CO_2 storage availability might allow for a more extensive use of natural gas coupled with CO_2 capture systems, while the opposite would introduce further stresses on the power sector to increase RES generation and green hydrogen production. On the other hand, stricter requirements on the share of domestic production of liquid fuels may lead to a shift of biomass uses towards biofuel production and/or to a higher production of e-fuels, with corresponding increases of hydrogen and carbon–neutral CO_2 consumption.

The assessment considers two scenario variants, modifying either the upper boundary of the CO_2 storage capacity or the limit on the import of liquid fuels. Specifically, the sensitivity analysis assumes an increase of the CO_2 storage capacity from 20 Mt_{CO2}/y to 40 Mt_{CO2}/y, corresponding to the upper boundary provided by the Italian LTS [105]. Conversely, liquid fuel import is limited to account for 60% of the national demand, in contrast to the value of 90% considered in the baseline scenario (i.e., 92 TWh_{LHV}/y instead of 138 TWh_{LHV}/y). Results in terms of variation with respect to the baseline scenario are summarised in Table 9 and discussed in the following sections.

5.1. Available CO_2 storage capacity

Results of the sensitivity analysis show that the system saturates the larger available capacity (40 Mt_{CO2}/y), further exploiting CO_2 capture systems. Specifically, CCS implementation on thermoelectric power generation plants starts to appear as a viable solution (see Table 10), compared to the baseline scenario, in which the sequestration capacity was hardly sufficient to contain the amount captured from cement production and primary steelmaking. This allows for an increase of natural gas consumption (+1130%, 130 TWh_{LHV}/y compared to 56 TWh_{LHV}/y) and a decrease in hydrogen consumption (-24%).

Table 10
Comparison of CO_2 capture and sequestration between the baseline scenario and the sensitivity analysis on the increase of available CO_2 storage capacity.

Item	Baseline scenario	Sensitivity
CO_2 capture on biogas upgrading	4 Mt_{CO2}/y	8 Mt_{CO2}/y
CO_2 capture on power generation	0 Mt_{CO2}/y	15 Mt_{CO2}/y
CO_2 capture on SMR	0 Mt_{CO2}/y	0 Mt_{CO2}/y
CO_2 capture on primary steelmaking	3 Mt_{CO2}/y	3 Mt_{CO2}/y
CO_2 capture on cement production	15 Mt_{CO2}/y	15 Mt_{CO2}/y
CO_2 to permanent sequestration	20 Mt_{CO2}/y	40 Mt_{CO2}/y
CO_2 use	2 Mt_{CO2}/y	1 Mt_{CO2}/y

Nevertheless, natural gas use remains significantly lower compared to today's status (approximately 700 TWh_{LHV}/y), and hydrogen continues having a relevant role in the integrated energy system, with a consumption that exceeds 230 TWh_{LHV}/y.

The observed behaviour has a twofold effect of reduction on the required RES power capacity, since a higher share of electricity demand is covered by thermoelectric generation and electrolysis consumption is reduced. In addition, the larger availability of cost-effective low-carbon electricity provides access to greater amounts of biomass for biofuel production, which undergoes a +13% increase compared to the baseline scenario. Consistently, e-fuel production experiences a corresponding decrease, further reducing the need for green hydrogen. From an economic perspective, a wider CO_2 storage capacity improves the system performance, yielding a 1% reduction of the total annual cost.

5.2. Limit on the import of liquid fuels

When introducing a stricter limit on liquid fuel import, the system adapts by massively increasing e-fuel production (+1130% compared to the baseline scenario), which becomes now prevalent with respect to that of biofuels. As expected, import is exploited up to the imposed limit, which now accounts for 60% of the total demand (92 TWh_{LHV}/y over 153 TWh_{LHV}/y) and consists entirely of carbon–neutral fuels. Biofuel production accounts for 28 TWh_{LHV}/y and saturates the entire biomass availability, requiring e-fuels to cover the residual demand of 33 TWh_{LHV}/y. This entails a 14% increase of hydrogen consumption, supported by a massive increase of RES power generation capacity (+20% of photovoltaic and +4% of onshore wind). Compared to the baseline scenario, the system exploits CCS on power generation (5 Mt_{CO2}/y) to adapt to the absence of carbon–neutral electricity from biomass power plants. Overall, stricter requirements on energy independence worsen the economic performance of the system, yielding a +1% increase of the total annual cost.

The system continues avoiding the use of direct air capture, as the required neutral CO_2 (11 Mt_{CO2}/y) is entirely of biogenic origin. However, even more stringent requirements on energy independency would likely entail the involvement of such option. Indeed, the maximum e-fuel production from biogenic CO_2 ranges between 60 and 125 TWh_{LHV}/y depending on whether biomass is exploited for biofuel production or as a source of biogenic CO_2. As a result, the system would require 9–30 Mt_{CO2}/y from DAC systems in order to cover the whole liquid fuel demand through domestic production, corresponding to an additional electricity consumption of 23–76 TWh_e/y. As an example, this would require the additional installation of approximately 20–70 GW_e of photovoltaic or 12–40 GW_e of onshore wind, further bringing the system towards the saturation of the available RES potential.

6. Areas for further development

The generalised formulation of OMNI-ES presented in this article will serve as a basis for further developments of the model, aimed at enhancing the level of detail of the analysis. Envisioned upgrades include the endogenous technology selection in relevant sectors (e.g., building heating and industrial heat generation), the introduction of ramping constraints and ancillary services provision, and the implementation of additional storage and network capabilities.

Depending on the case study, the model structure allows for the broadening of the spectrum of included technologies. For example, nuclear power generation was not considered in this work since it is not currently present in Italy nor it is envisioned by national development plans [105], but could be introduced when assessing a different case study.

The analysed Italian case study mainly serves as an example of model application. As the modelling framework development is the primary focus of this work, minor attention has been given to the scenario definition and to the discussion of the underlying assumptions, as this

will be the focus of follow-up works that will apply OMNI-ES to assess alternative scenarios and provide policy recommendations regarding the achievement of economy-wide decarbonisation in Italy. Such assessment will also extend the sensitivity analyses and enlarge the technological options (e.g., larger attention on floating wind if the potential in the difficult seawater conditions emerges) in order to discuss conflicting or synergistic impacts of boundary conditions (e.g., import limits, weather years) and techno-economic parameters.

7. Conclusions

This article presented the OMNI-ES framework, a novel bottom-up modelling tool for the techno-economic optimisation of a highly integrated national energy system, based on a multi-node formulation and on an hourly-resolved temporal resolution. With respect to the existing literature, OMNI-ES develops a truly comprehensive approach, which is essential for the study of carbon–neutral scenarios. Among the novelties, a crucial feature is the co-presence of multiple energy vectors, including electricity, gas (with the possibility of blending methane and hydrogen), hydrogen, and liquid fuels, together with the related transport networks. In addition, sector integration is accurately represented by considering the inter-relations between the energy vectors and the demands from all sectors. These include residential and services, road mobility, aviation, navigation, and industry. The latter considers process heat generation, feedstocks for the chemical industries, and heavy industrial activities (i.e., primary steelmaking and cement production). Finally, the net-zero emission constraint is implemented by tracking direct and indirect CO_2 flows, encompassing carbon sources, sinks, and usages, with a closure term that highlights the possible need for additional or externalised CO_2 damping support.

As a case study, OMNI-ES is applied to investigate a long-term scenario for Italy capable to reach net-zero CO_2 emissions, considering 2050 as target year. In a carbon–neutral perspective, the case of Italy serves as a noteworthy example, as the country must switch from a system that is mostly based on imports of fossil fuels (especially natural gas and oil-based liquid fuels), and renewable sources are unevenly distributed in the territory. In addition, considering Italy's strategic position as gateway between North Africa and Europe, the development of adequate infrastructures will be crucial to enable the creation of a bridge between the two regions.

Although results should not be treated as projections nor exact estimates, they are relevant as they offer a numerical understanding of the scale and orders of magnitude of the technical and economic requirements. Within the framework of studies focusing on the future Italian energy system [42,48,105], results of the present analysis show that, when considering the economy-wide decarbonisation, the capacity needs of RES power generation and storage system should be revised upward. Specifically, the cost-optimal, carbon–neutral energy system requires 15–20 times today's renewable capacity exceeding 300 GW_e of photovoltaic and 130 GW_e of onshore wind, as well as a spread presence of flexibility elements, in the form of storage or dispatchable plants. Short-term oscillations of renewable power output are covered by battery energy storage systems, which feature an installed capacity of over 110 GWh_e and are cycled on a daily basis. On the other hand, pumped hydro and underground hydrogen storage are employed to compensate seasonal mismatches, as they are characterised by large installed capacities (779 GWh_e and 883 GWh_{LHV}, respectively) and few equivalent operating cycles per year (17 and 16, respectively). In addition, hydrogen acts as enabler of sector coupling, integrating the power sector with the end-use sectors, through either direct use, injection in the gas grid, or conversion into other energy vectors (e-fuels, or reconversion to electricity).

Biogenic sources emerge as critical elements in the system, enabling the generation of carbon–neutral vectors (electricity, methane, and liquid fuels). However, their limited availability causes a strong competition between sectors for their use. If the import limit of carbon–neutral liquid fuels is not excessively stringent, biomass uses favour power generation over biofuel production. On the contrary, the latter is prioritised up to saturation of the biomass availability when a higher degree of energy independence is imposed. E-fuel production becomes relevant only when the entire biofuel potential is exploited, and it introduces further stresses on the power sector due the additional requests for green hydrogen and neutral CO_2. In general, although a significant number of ESMs disregards the role of liquid fuels in long-term scenarios, the constraints on their origin are among the most impactful on the energy system configuration. Moreover, domestic production can become a relevant aspect considering that the availability and cost of carbon–neutral LF import are likely to suffer from a strong global competition. Indeed, most countries will face the need for carbon–neutral liquid fuels in a context of limited biomass availability for biofuels and of high impact of electricity requirements for H_2 and neutral CO_2 provision for e-fuels.

The fine spatial resolution implemented in OMNI-ES enables the identification of inter-regional energy vector exchanges (the 20 nodes in the case study correspond to NUTS-2 level areas). The capacity of the existing gas grid, repurposed to deliver a blend of methane and hydrogen, is saturated, requiring the development of a dedicated hydrogen delivery infrastructure. Specifically, the gas grid delivers 115 TWh_{LHV}/y of hydrogen and 110 TWh_{LHV}/y of methane, while over 240 TWh_{LHV}/y of hydrogen are delivered through the hydrogen infrastructure, including 50 TWh_{LHV}/y that are imported from North Africa and exported to northern Europe. Overall, hydrogen transport features south-north corridors to supply the main consumption areas in northern region and to meet the export requirements to northern European countries.

The system achieves carbon neutrality by saturating the assumed limit of CO_2 storage capacity of 20 Mt_{CO2}/y, implementing CO_2 capture on both fossil and biogenic sources. Permanent sequestration appears essential to both compensate unavoidable emissions and reduce process-related emissions in hard-to-abate industries (e.g., primary steelmaking and cement production). Regarding the production of carbon–neutral fuels, biogenic CO_2 is favoured over direct air capture, as the latter is both more capital- and energy-intensive.

Overall, the model application suggests that considering the demand of the various energy vectors in all sectors in an integrated manner is crucial, since exclusions correspond to an underestimation of the technical requirements and to a virtual overestimation of sources availability. Significant examples are hard-to-abate activities, such as aviation, navigation, and heavy industries, which are overlooked in numerous studies, despite being major sources of emissions. Considering the limited availability of sources and the complex set of interactions that underpin the integrated energy system, the identification of the optimal configuration and operation is not trivial. Accordingly, energy system models should include all the available decarbonisation options for each sector in terms of both energy vectors and technologies, as predetermined exclusions may be detrimental to the system performance. With the massive deployment of carbon–neutral energy vectors, transport networks have a critical role. As such, models should be capable of representing all networks, in order to account for possible bottlenecks and to identify infrastructural development requirements. In this perspective, the gas network is of particular relevance, as it offers the possibility to deliver carbon–neutral energy vectors exploiting existing infrastructures. In conclusion, it is only when all these characteristics are combined that carbon–neutral energy systems can be investigated with a truly integrated and comprehensive approach, enabling crucial understanding of the optimal configuration and operation.

CRediT authorship contribution statement

Paolo Colbertaldo: Conceptualization, Methodology, Software, Data curation, Investigation, Validation, Writing – original draft, Writing – review & editing. **Federico Parolin:** Software, Data curation,

Investigation, Visualization, Methodology, Writing – original draft. **Stefano Campanari:** Conceptualization, Supervision, Writing – review & editing.

Declaration of Competing Interest

The authors declare that they have no known competing financial interests or personal relationships that could have appeared to influence the work reported in this paper.

Data availability

Data will be made available on request.

Acknowledgements

The authors thankfully acknowledge the RELab research group at the Department of Energy of Politecnico di Milano, and in particular Dr. Fabrizio Fattori, Ms. Marianna Pozzi, Mr. Francesco Mezzera, and Mr. Lorenzo Cassetti, for the support in the development of input data regarding heating and cooling demand and related hourly profiles as well as in the definition of the biomass potential of the Italian regions. The authors also acknowledge the same group and the Hydrogen Joint Research Platform (H2 JRP) partners for the fruitful discussions regarding the simulation needs of the integrated Italian case study.

Appendix A. Supplementary data

Supplementary data to this article can be found online at https://doi.org/10.1016/j.enconman.2023.117168.

References

[1] NewClimate Institute, Oxford Net Zero. Energy & Climate Intelligence Unit, Data-Driven EnviroLab, Net zero stocktake. 2022.
[2] IEA, Net Zero by 2050, 2021.
[3] IRENA, State Grid Corporation of China, Electrification with Renewables: Driving the transformation of energy services, 2019.
[4] Fuel Cells and Hydrogen Joint Undertaking (FCH), Hydrogen Roadmap Europe, 2019. https://doi.org/10.2843/249013.
[5] Shell, Deloitte, Decarbonising Aviation: Cleared for Take-Off, 2021.
[6] IRENA, A pathway to decarbonise the shipping sector by 2050, 2021.
[7] IRENA, Renewable Energy Policies in a Time of Transition. Heating and Cooling, 2020.
[8] Madeddu S, Ueckerdt F, Pehl M, Peterseim J, Lord M, Kumar KA, et al. The CO2 reduction potential for the European industry via direct electrification of heat supply (power-to-heat). Environ Res Lett 2020;15(12):124004.
[9] A.M. Bazzanella, F. Ausfelder, DECHEMA, Low carbon energy and feedstock for the European chemical industry, 2017.
[10] Lopion P, Markewitz P, Robinius M, Stolten D. A review of current challenges and trends in energy systems modeling. Renew Sustain Energy Rev 2018;96:156–66. https://doi.org/10.1016/j.rser.2018.07.045.
[11] Ringkjøb HK, Haugan PM, Solbrekke IM. A review of modelling tools for energy and electricity systems with large shares of variable renewables. Renew Sustain Energy Rev 2018;96:440–59. https://doi.org/10.1016/j.rser.2018.08.002.
[12] Prina MG, Manzolini G, Moser D, Nastasi B, Sparber W. Classification and challenges of bottom-up energy system models - A review. Renew Sustain Energy Rev 2020;129:109917.
[13] Fodstad M, Crespo del Granado P, Hellemo L, Knudsen BR, Pisciella P, Silvast A, et al. Next frontiers in energy system modelling: A review on challenges and the state of the art. Renew Sustain Energy Rev 2022;160:112246.
[14] Bussar C, Stöcker P, Cai Z, Moraes L, Magnor D, Wiernes P, et al. Large-scale integration of renewable energies and impact on storage demand in a European renewable power system of 2050-Sensitivity study. J Energy Storage 2016;6:1–10. https://doi.org/10.1016/j.est.2016.02.004.
[15] M. Francesco, F. Fabrizio, M. Mario, NEMeSI (National Energy Model for a Sustainable Italy) 2050 version, (2020). https://doi.org/10.5281/ZENODO.4271832.
[16] Koirala B, Hers S, Morales-España G, Özdemir Ö, Sijm J, Weeda M. Integrated electricity, hydrogen and methane system modelling framework: Application to the Dutch Infrastructure Outlook 2050. Appl Energy 2021;289. https://doi.org/10.1016/j.apenergy.2021.116713.
[17] Prina MG, Moser D, Vaccaro R, Sparber W. EPLANopt optimization model based on EnergyPLAN applied at regional level: The future competition on excess electricity production from renewables. Int J Sustain Energy Plan Manag 2020;27:35–50. https://doi.org/10.5278/ijsepm.3504.
[18] Prina MG, Lionetti M, Manzolini G, Sparber W, Moser D. Transition pathways optimization methodology through EnergyPLAN software for long-term energy planning. Appl Energy 2019;235:356–68. https://doi.org/10.1016/j.apenergy.2018.10.099.
[19] Prina MG, Casalicchio V, Kaldemeyer C, Manzolini G, Moser D, Wanitschke A, et al. Multi-objective investment optimization for energy system models in high temporal and spatial resolution. Appl Energy 2020;264. https://doi.org/10.1016/j.apenergy.2020.114728.
[20] Lund H, Thellufsen JZ, Østergaard PA, Sorknæs P, Skov IR, Mathiesen BV. EnergyPLAN – Advanced analysis of smart energy systems. Smart Energy 2021;1:100007. https://doi.org/10.1016/j.segy.2021.100007.
[21] Lopez G, Aghahosseini A, Child M, Khalili S, Fasihi M, Bogdanov D, et al. Impacts of model structure, framework, and flexibility on perspectives of 100% renewable energy transition decision-making. Renew Sustain Energy Rev 2022;164:112452. https://doi.org/10.1016/j.rser.2022.112452.
[22] DeCarolis JF, Babaee S, Li B, Kanungo S. Modelling to generate alternatives with an energy system optimization model. Environ Model Softw 2016;79:300–10. https://doi.org/10.1016/j.envsoft.2015.11.019.
[23] Victoria M, Zhu K, Brown T, Andresen GB, Greiner M. Early decarbonisation of the European energy system pays off. Nat Commun 2020;11:1–9. https://doi.org/10.1038/s41467-020-20015-4.
[24] Colbertaldo P, Cerniauskas S, Grube T, Robinius M, Stolten D, Campanari S. Clean mobility infrastructure and sector integration in long-term energy scenarios: The case of Italy. Renew Sustain Energy Rev 2020;133:110086. https://doi.org/10.1016/j.rser.2020.110086.
[25] Pickering B, Lombardi F, Pfenninger S. Diversity of options to eliminate fossil fuels and reach carbon neutrality across the entire European energy system. Joule 2022;6:1253–76. https://doi.org/10.1016/j.joule.2022.05.009.
[26] Tröndle T, Lilliestam J, Marelli S, Pfenninger S. Trade-Offs between Geographic Scale. Cost, and Infrastructure Requirements for Fully Renewable Electricity in Europe, Joule 2020;4:1929–48. https://doi.org/10.1016/j.joule.2020.07.018.
[27] Simoes S, Nijs W, Ruiz P, Sgobbi A, Radu D, Bolat P, et al. The JRC-EU-TIMES model 2013. https://doi.org/10.2790/97596.
[28] Lombardi F, Pickering B, Colombo E, Pfenninger S. Policy Decision Support for Renewables Deployment through Spatially Explicit Practically Optimal Alternatives. Joule 2020;4:2185–207. https://doi.org/10.1016/j.joule.2020.08.002.
[29] Victoria M, Zeyen E, Brown T. Speed of technological transformations required in Europe to achieve different climate goals. Joule 2022;6:1066–86. https://doi.org/10.1016/J.JOULE.2022.04.016.
[30] F. Neumann, E. Zeyen, M. Victoria, T. Brown, Benefits of a Hydrogen Network in Europe, Preprint. (2022).
[31] Wiese F, Bramstoft R, Koduvere H, Pizarro Alonso A, Balyk O, Kirkerud JG, et al. Balmorel open source energy system model, Energy. Strateg Rev 2018;20:26–34. https://doi.org/10.1016/j.esr.2018.01.003.
[32] Jensen IG, Wiese F, Bramstoft R, Münster M. Potential role of renewable gas in the transition of electricity and district heating systems. Energy Strateg Rev 2020;27:100446.
[33] J. Gea-Bermúdez, I.G. Jensen, M. Münster, M. Koivisto, J.G. Kirkerud, Y. kuang Chen, H. Ravn, The role of sector coupling in the green transition: A least-cost energy system development in Northern-central Europe towards 2050, Appl. Energy. 289 (2021). https://doi.org/10.1016/j.apenergy.2021.116685.
[34] Bramstoft R, Pizarro-Alonso A, Jensen IG, Ravn H, Münster M. Modelling of renewable gas and renewable liquid fuels in future integrated energy systems. Appl Energy 2020;268:114869. https://doi.org/10.1016/j.apenergy.2020.114869.
[35] Barrett M, Spataru C. DynEMo: A Dynamic Energy Model for the Exploration of Energy, Society and Environment. In: Proc. - UKSim-AMSS 17th Int. Conf. Comput. Model. Simulation, UKSim 2015. Institute of Electrical and Electronics Engineers Inc.; 2016. p. 255–60. https://doi.org/10.1109/UKSim.2015.104.
[36] Backe S, Skar C, del Granado PC, Turgut O, Tomasgard A. EMPIRE: An open-source model based on multi-horizon programming for energy transition analyses. SoftwareX 2022;17:100877. https://doi.org/10.1016/j.softx.2021.100877.
[37] Lund H, Skov IR, Thellufsen JZ, Sorknæs P, Korberg AD, Chang M, et al. The role of sustainable bioenergy in a fully decarbonised society. Renew Energy 2022;196:195–203. https://doi.org/10.1016/j.renene.2022.06.026.
[38] Lund H, Thellufsen JZ, Sorknæs P, Mathiesen BV, Chang M, Madsen PT, et al. A consistent and detailed strategy for a fully decarbonized society, Renew. Sustain Energy Rev 2022;168:112777. https://doi.org/10.1016/j.rser.2022.112777.
[39] Battaglia V, De Luca G, Fabozzi S, Lund H, Vanoli L. Integrated energy planning to meet 2050 European targets: A Southern Italian region case study. Energy Strateg Rev 2022;41:100844. https://doi.org/10.1016/j.esr.2022.100844.
[40] Bellocchi S, Manno M, Noussan M, Prina MG, Vellini M. Electrification of transport and residential heating sectors in support of renewable penetration: Scenarios for the Italian energy system. Energy 2020;196:117062. https://doi.org/10.1016/j.energy.2020.117062.
[41] Bellocchi S, Colbertaldo P, Manno M, Nastasi B. Assessing the effectiveness of hydrogen pathways: A techno-economic optimisation within an integrated energy system. Energy 2023;263:126017. https://doi.org/10.1016/j.energy.2022.126017.
[42] Bellocchi S, De Falco M, Gambini M, Manno M, Stilo T, Vellini M. Opportunities for power-to-Gas and Power-to-liquid in CO2-reduced energy scenarios: The Italian case. Energy 2019;175:847–61. https://doi.org/10.1016/j.energy.2019.03.116.

[43] Limpens G, Moret S, Jeanmart H, Maréchal F. EnergyScope TD: A novel open-source model for regional energy systems. Appl Energy 2019;255:113729. https://doi.org/10.1016/j.apenergy.2019.113729.

[44] Borasio M, Moret S. Deep decarbonisation of regional energy systems: A novel modelling approach and its application to the Italian energy transition. Renew Sustain Energy Rev 2022;153:111730. https://doi.org/10.1016/j.rser.2021.111730.

[45] Bernath C, Deac G, Sensfuß F. Influence of heat pumps on renewable electricity integration: Germany in a European context. Energy Strateg Rev 2019;26:100389. https://doi.org/10.1016/j.esr.2019.100389.

[46] Franke K, Sensfuß F, Bernath C, Lux B. Carbon-neutral energy systems and the importance of flexibility options: A case study in China. Comput Ind Eng 2021;162:107712. https://doi.org/10.1016/j.cie.2021.107712.

[47] Shirizadeh B, Quirion P. The importance of renewable gas in achieving carbon-neutrality: Insights from an energy system optimization model. Energy 2022;255:124503. https://doi.org/10.1016/j.energy.2022.124503.

[48] Prina MG, Fornaroli FC, Moser D, Manzolini G, Sparber W. Optimisation method to obtain marginal abatement cost-curve through EnergyPLAN software. Smart Energy 2021;1:100002. https://doi.org/10.1016/j.segy.2021.100002.

[49] C. Heaton, Modelling Low-Carbon Energy System Designs with the ETI ESME Model, 2014.

[50] Caglayan DG, Heinrichs HU, Robinius M, Stolten D. Robust design of a future 100% renewable european energy supply system with hydrogen infrastructure. Int J Hydrogen Energy 2021;46:29376–90. https://doi.org/10.1016/j.ijhydene.2020.12.197.

[51] Burandt T, Xiong B, Löffler K, Oei P-Y. Decarbonizing China's energy system – Modeling the transformation of the electricity, transportation, heat, and industrial sectors. Appl Energy 2019;255:113820. https://doi.org/10.1016/j.apenergy.2019.113820.

[52] Löffler K, Hainsch K, Burandt T, Oei P-Y, Kemfert C, von Hirschhausen C. Designing a model for the global energy system-GENeSYS-MOD: An application of the Open-Source Energy Modeling System (OSeMOSYS). Energies 2017;10(10):1468. https://doi.org/10.3390/en10101468.

[53] Rinaldi A, Yilmaz S, Patel MK, Parra D. What adds more flexibility? An energy system analysis of storage, demand-side response, heating electrification, and distribution reinforcement. Renew Sustain Energy Rev 2022;167:112696. https://doi.org/10.1016/j.rser.2022.112696.

[54] Feijoo F, Pfeifer A, Herc L, Groppi D, Duić N. A long-term capacity investment and operational energy planning model with power-to-X and flexibility technologies. Renew Sustain Energy Rev 2022;167:112781. https://doi.org/10.1016/j.rser.2022.112781.

[55] C.G. Heaps, LEAP: The Low Emissions Analysis Platform. [Software version: 2020.1.76], 2022.

[56] McPherson M, Karney B. Long-term scenario alternatives and their implications: LEAP model application of Panama's electricity sector. Energy Policy 2014;68:146–57. https://doi.org/10.1016/j.enpol.2014.01.028.

[57] Ghanadan R, Koomey JG. Using energy scenarios to explore alternative energy pathways in California. Energy Policy 2005;33:1117–42. https://doi.org/10.1016/j.enpol.2003.11.011.

[58] Bogdanov D, Farfan J, Sadovskaia K, Aghahosseini A, Child M, Gulagi A, et al. Radical transformation pathway towards sustainable electricity via evolutionary steps. Nat Commun 2019;10. https://doi.org/10.1038/s41467-019-08855-1.

[59] Bogdanov D, Gulagi A, Fasihi M, Breyer C. Full energy sector transition towards 100% renewable energy supply: Integrating power, heat, transport and industry sectors including desalination. Appl Energy 2021;283:116273. https://doi.org/10.1016/j.apenergy.2020.116273.

[60] IIASA. Model for Energy Supply Strategy Alternatives and their General Environmental Impact (MESSAGE). 2012.

[61] Sakellaris K, Canton J, Zafeiratou E, Fournié L. METIS – An energy modelling tool to support transparent policy making, Energy. Strateg Rev 2018;22:127–35. https://doi.org/10.1016/j.esr.2018.08.013.

[62] Fattori F, Tagliabue L, Cassetti G, Motta M. Enhancing Power System Flexibility Through District Heating - Potential Role in the Italian Decarbonisation. In: Conf. Proceedings, 2019 IEEE Int. Conf. Environ. Electr. Eng. and 2019 IEEE Ind. Commer. Power Syst. Eur; 2019. https://doi.org/10.1109/EEEIC.2019.8783732.

[63] Fattori F, Tagliabue L, Cassetti G, Motta M. NEMeSI (National Energy Model for a Sustainable Italy). 2019. https://doi.org/10.5281/zenodo.2654871.

[64] Mezzera F, Fattori F, Dénarié A, Motta M. Waste-heat utilization potential in a hydrogen-based energy system - an exploratory focus on Italy. Int J Sustain Energy Plan Manag 2021;31:95–108. https://doi.org/10.5278/ijsepm.6292.

[65] Elberry AM, Thakur J, Veysey J. Seasonal hydrogen storage for sustainable renewable energy integration in the electricity sector: A case study of Finland. J Energy Storage 2021;44:103474. https://doi.org/10.1016/j.est.2021.103474.

[66] Barbosa J, Ripp C, Steinke F. Accessible modeling of the German energy transition: An open, compact, and validated model. Energies 2021;14(23):8084. https://doi.org/10.3390/en14238084.

[67] Harewood A, Dettner F, Hilpert S. Open source modelling of scenarios for a 100% renewable energy system in Barbados incorporating shore-to-ship power and electric vehicles, Energy. Sustain Dev 2022;68:120–30. https://doi.org/10.1016/j.esd.2022.03.004.

[68] Hilpert S, Dettner F, Al-Salaymeh A. Analysis of cost-optimal renewable energy expansion for the near-term jordanian electricity system. Sustain 2020;12:1–21. https://doi.org/10.3390/su12229339.

[69] Maruf MNI. Open model-based analysis of a 100% renewable and sector-coupled energy system–The case of Germany in 2050. Appl Energy 2021;288:116618. https://doi.org/10.1016/j.apenergy.2021.116618.

[70] Henke HTJ, Gardumi F, Howells M. The open source electricity Model Base for Europe - An engagement framework for open and transparent European energy modelling. Energy 2022;239:121973. https://doi.org/10.1016/j.energy.2021.121973.

[71] Howells M, Rogner H, Strachan N, Heaps C, Huntington H, Kypreos S, et al. OSeMOSYS: The Open Source Energy Modeling System. An introduction to its ethos, structure and development. Energy Policy 2011;39:5850–70. https://doi.org/10.1016/j.enpol.2011.06.033.

[72] S. Motalebi, T. Barnes, S. Kaspar, A.S. Wright, T. Niet, Hydrogen to Provide Flexibility in The Canadian Energy System, 2021.

[73] Deane JP, Ciaráin MÓ, Gallachóir BPÓ. An integrated gas and electricity model of the EU energy system to examine supply interruptions. Appl Energy 2017;193:479–90. https://doi.org/10.1016/j.apenergy.2017.02.039.

[74] K. Keramidas, A. Kitous, J. Schmitz, POLES-JRC model documentation 2017 EUR 28728 EN, 2017. https://doi.org/10.2760/225347.

[75] E3Modelling, PRIMES MODEL. VERSION 2018. Detailed model description, 2018.

[76] Brown T, Schlachtberger D, Kies A, Schramm S, Greiner M. Synergies of sector coupling and transmission reinforcement in a cost-optimised, highly renewable European energy system. Energy 2018;160:720–39. https://doi.org/10.1016/j.energy.2018.06.222.

[77] Pedersen TT, Victoria M, Rasmussen MG, Andresen GB. Modeling all alternative solutions for highly renewable energy systems. Energy 2021;234:121294. https://doi.org/10.1016/j.energy.2021.121294.

[78] Baumstark L, Bauer N, Benke F, Bertram C, Bi S, Gong CC, et al. REMIND2.1: transformation and innovation dynamics of the energy-economic system within climate and sustainability limits. Geosci. Model Dev. 2021;14:6571–603. https://doi.org/10.5194/gmd-14-6571-2021.

[79] Gils HC, Scholz Y, Pregger T, de Tena DL, Heide D. Integrated modelling of variable renewable energy-based power supply in Europe. Energy 2017;123:173–88. https://doi.org/10.1016/j.energy.2017.01.115.

[80] Michalski J, Bünger U, Crotogino F, Donadei S, Schneider GS, Pregger T, et al. Hydrogen generation by electrolysis and storage in salt caverns: Potentials, economics and systems aspects with regard to the German energy transition. Int J Hydrogen Energy 2017;42:13427–43. https://doi.org/10.1016/j.ijhydene.2017.02.102.

[81] Gils HC, Gardian H, Schmugge J. Interaction of hydrogen infrastructures with other sector coupling options towards a zero-emission energy system in Germany. Renew Energy 2021;180:140–56. https://doi.org/10.1016/j.renene.2021.08.016.

[82] Henning HM, Palzer A. A comprehensive model for the German electricity and heat sector in a future energy system with a dominant contribution from renewable energy technologies - Part I: Methodology. Renew Sustain Energy Rev 2014;30:1003–18. https://doi.org/10.1016/j.rser.2013.09.012.

[83] Sterchele P, Kersten K, Palzer A, Hentschel J, Henning H-M. Assessment of flexible electric vehicle charging in a sector coupling energy system model – Modelling approach and case study. Appl Energy 2020;258:114101. https://doi.org/10.1016/j.apenergy.2019.114101.

[84] Kost C, Brandes J, Senkpiel C, Sterchele P, Wrede D, Henning H-M. Modeling of persistence, non-acceptance and sufficiency in long-term energy scenarios for Germany. Energies 2021;14(15):4484. https://doi.org/10.3390/en14154484.

[85] Hunter K, Sreepathi S, DeCarolis JF. Modeling for insight using Tools for Energy Model Optimization and Analysis (Temoa). Energy Econ 2013;40:339–49. https://doi.org/10.1016/j.eneco.2013.07.014.

[86] Dorfner J. Open Source Modelling and Optimisation of Energy Infrastructure at Urban Scale. Technische Universität München. Technische Universität München; 2015.

[87] IEA. World Energy Model Documentation. 2021.

[88] Colbertaldo P, Guandalini G, Campanari S. Modelling the integrated power and transport energy system: The role of power-to-gas and hydrogen in long-term scenarios for Italy. Energy 2018;154:592–601. https://doi.org/10.1016/j.energy.2018.04.089.

[89] Colbertaldo P, Agustin SB, Campanari S, Brouwer J. Impact of hydrogen energy storage on California electric power system: Towards 100% renewable electricity. Int J Hydrogen Energy 2019;44:9558–76. https://doi.org/10.1016/j.ijhydene.2018.11.062.

[90] Colbertaldo P, Guandalini G, Crespi E, Campanari S. Balancing a high-renewables electric grid with hydrogen-fuelled combined cycles: A contry scale analysis. Proc. ASME Turbo Expo. 2020. https://doi.org/10.1115/GT2020-15570. GT2020-15570, 2020.

[91] S. Pfenninger, B. Pickering, Calliope: a multi-scale energy systems modelling framework, J. Open Source Softw. 3 (2018) 825. https://doi.org/10.21105/joss.00825.

[92] Hilpert S, Kaldemeyer C, Krien U, Günther S, Wingenbach C, Plessmann G. The Open Energy Modelling Framework (oemof) - A new approach to facilitate open science in energy system modelling, Energy. Strateg Rev 2018;22:16–25. https://doi.org/10.1016/j.esr.2018.07.001.

[93] J. Lofberg, YALMIP : A toolbox for modeling and optimization in MATLAB, 2004 IEEE Int. Conf. Robot. Autom. (IEEE Cat. No.04CH37508). (2004) 284–289. https://doi.org/doi: 10.1109/CACSD.2004.1393890.

[94] Gurobi Optimization, Gurobi Optimizer reference manual, 2014.

[95] IBM ILOG CPLEX Optimization Studio CPLEX User's Manual.

[96] Terna, Snam Rete Gas, Documento di Descrizione degli Scenari, 2022.

[97] Entso-E, Total Load - 2019.

[98] Terna, Regional demand data, 2019.

[99] Ministero dell'Ambiente e della Sicurezza Energetica, Energy and mining statistics - Natural gas, 2019.
[100] Pozzi M, Spirito G, Fattori F, Dénarié A, Famiglietti J, Motta M. Synergies between buildings retrofit and district heating. The role of DH in a decarbonized scenario for the city of Milano, Energy Reports 2021;7:449–57. https://doi.org/10.1016/j.egyr.2021.08.083.
[101] Dénarié A, Fattori F, Spirito G, Macchi S, Cirillo VF, Motta M, et al. Assessment of waste and renewable heat recovery in DH through GIS mapping: The national potential in Italy. Smart Energy 2021;1:100008. https://doi.org/10.1016/J.SEGY.2021.100008.
[102] Dehghan BB, Toppi T, Aprile M, Motta M. Seasonal performance assessment of three alternative gas-driven absorption heat pump cycles. J Build Eng 2020;31:101434. https://doi.org/10.1016/j.jobe.2020.101434.
[103] IRENA, Reaching Zero With Renewables, 2020.
[104] Colbertaldo P, Guandalini G, Campanari S. Development of benchmark scenarios for sector coupling in the Italian national energy system for 100% RES supply to power and mobility. E3S Web Conf 2021;312:01003. https://doi.org/10.1051/e3sconf/202131201003.
[105] Ministero dell'Ambiente e della Tutela del Territorio e del Mare, Ministero dello Sviluppo Economico, Ministero delle Infrastrutture e dei Trasporti, Ministero delle Politiche agricole Alimentari e Forestali. Strategia italiana di lungo termine sulla riduzione delle emissioni dei gas a effetto serra; 2021 https://ec.europa.eu/clima/sites/lts/lts_it_it.pdf.
[106] ANAV, Primo rapporto sul mercato del noleggio autobus con conducente e il trasporto turistico, 2018.
[107] Ruf Y, Kaufmann M, Lange S, Pfister J, Heieck F, Endres Brussels A. Fuel Cells and Hydrogen Applications for European Regions and Cities 2017.
[108] Ruf Y, Baum M, Zorn T, Menzel A, Rehberger J. Fuel Cell Hydrogen Trucks - Heavy-Duty's High Performance Green Solution 2020.
[109] Powell N, Hill N, Bates J, Bottrell N, Biedka M, White B, et al. Impact Analysis of Mass EV Adoption and Low Carbon Intensity Fuels Scenarios. 2018.
[110] Ministero delle Infrastrutture e della Mobilità Sostenibili, Conto Nazionale delle Infrastrutture e della Mobilità Sostenibili - Anni 2019-2020, 2019.
[111] UNRAE, GiPA, L'autotrasporto italiano nel contesto europeo: dinamiche e prospettive, 2018.
[112] Unione Petrolifera, Previsioni domanda energetica e petrolifera 2019-2040, 2019.
[113] DNV, Maritime forecast to 2050, 2022.
[114] GSE, Energia nel settore trasporti 2005-2020, 2021.
[115] Assaeroporti, Annual data, 2019.
[116] Assoporti, Statistics, 2019.
[117] Mantzos L, Matei N, Mulholland E, Rózsai M, Tamba M, Wiesenthal T. The JRC Integrated Database of the European Energy System. European Commission 2018.
[118] De Lena E, Arias B, Romano MC, Abanades JC. Integrated Calcium Looping System with Circulating Fluidized Bed Reactors for Low CO_2 Emission Cement Plants. Int J Greenh Gas Control 2022;114:103555. https://doi.org/10.1016/j.ijggc.2021.103555.
[119] IEA, Technology roadmap for cement; 2018.
[120] CEMBUREAU. Cementing the European Green Deal: REACHING CLIMATE NEUTRALITY ALONG THE CEMENT AND CONCRETE VALUE CHAIN BY 2050; 2020.
[121] ISTAT. Regional Structural Business Statistics. 2008. http://dati.istat.it/Index.aspx?DataSetCode=DCSP_SBSNAZ2002.
[122] Ministry of Economic Development. Ministry of the Environment and Protection of Natural Resources and the Sea, Ministry of Infrastructure and Transport. Integrated National Energy and Climate Plan; 2019.
[123] Decreto del. Presidente del Consiglio dei Ministri 10 agosto 2016. Gazz. Uff. della Repubb. Ital. 2016.
[124] Ministero dello Sviluppo Economico,. Data Book, 2020.
[125] R. Pudelko, M. Borzecka-Walker, A. Faber. The feedstock potential assessment for EU-27 + Switzerland in NUTS-3. Deliverable D1.2 of the BioBoost project, 2013.
[126] Ministero della Salute. Livestock Database 2019.
[127] European Hydrogen Backbone, Guidehouse, Five hydrogen supply corridors for Europe in 2030, 2022.
[128] European Commission, COMMUNICATION FROM THE COMMISSION TO THE EUROPEAN PARLIAMENT, THE EUROPEAN COUNCIL, THE COUNCIL, THE EUROPEAN ECONOMIC AND SOCIAL COMMITTEE AND THE COMMITTEE OF THE REGIONS REPowerEU: Joint European Action for more affordable, secure and sustainable energ, 2022.
[129] European Commision, Implementing the Repower EU action plan: Investment needs, hydrogen accelerator and achieving the bio-methane targets, 2022.
[130] Snam Rete Gas, Ten-Year Plan 2022-2031, 2022.
[131] Snam Rete Gas, Technical data for the network, 2016.
[132] Snam Rete Gas, Sustainability report 2021, 2021.
[133] Parolin F, Colbertaldo P, Campanari S. Development of a multi-modality hydrogen delivery infrastructure: An optimization model for design and operation. Energy Convers Manag 2022;266:115650. https://doi.org/10.1016/j.enconman.2022.115650.
[134] Parolin F, Colbertaldo P, Campanari S. Benefits of the multi-modality formulation in hydrogen supply chain modelling. E3S Web Conf 2022;334:02003. https://doi.org/10.1051/e3sconf/202233402003.
[135] HyUnder, Assessment of the potential, the actors and relevant business cases for large scale and seasonal storage of renewable electricity by hydrogen underground storage in Europe. Overview on all Known Underground Storage Technologies for Hydrogen, 2013.
[136] Snam Rete Gas, Daily capacity booking, 2019.
[137] Snam Rete Gas, LNG operational data, 2022.
[138] European Commission, EU Taxonomy Compass.
[139] M. Prussi, M. Yugo, L. De Prada, M. Padella, M. Edwards, JEC well-To-wheels report v5, 2020. https://doi.org/10.2760/100379.
[140] IRENA, Global hydrogen trade to meet the 1.5°C climate goal: Part III – Green hydrogen cost and potential, 2022.
[141] IEAGHG, Techno - Economic Evaluation of SMR Based Standalone (Merchant) Hydrogen Plant with CCS, 2017.
[142] Poluzzi A, Guandalini G, d'Amore F, Romano MC. The Potential of Power and Biomass-to-X Systems in the Decarbonization Challenge: a Critical Review. Curr Sustain Energy Reports 2021;8:242–52. https://doi.org/10.1007/s40518-021-00191-7.
[143] Ministero della Transizione Ecologica. Energy and mining analysis and statistics: Weekly fuel prices.
[144] ARERA, Relazione annuale 2020 sullo stato dei servizi e sull'attività svolta, 2021.
[145] DOE Hydrogen and Fuel Cell Technologies Office. Fuel Cell Technologies Office Multi-Year Research, Development, and Demonstration Plan, 3.2 Hydrogen Delivery; 2015.
[146] TNO, Power-2-Fuel Cost Analysis, 2020.
[147] Terna, Statistics 2019, 2019.
[148] Crespi E, Colbertaldo P, Guandalini G, Campanari S. Energy storage with Power-to-Power systems relying on photovoltaic and hydrogen: modelling the operation with secondary reserve provision. J Energy Storage 2022;55:105613. https://doi.org/10.1016/j.est.2022.105613.
[149] IEA, Italy: Key energy statistics, 2019.
[150] ISPRA, Le emissioni di gas serra in Italia alla fine del secondo periodo del Protocollo di Kyoto: obiettivi di riduzione ed efficienza energetica, 2022.